18

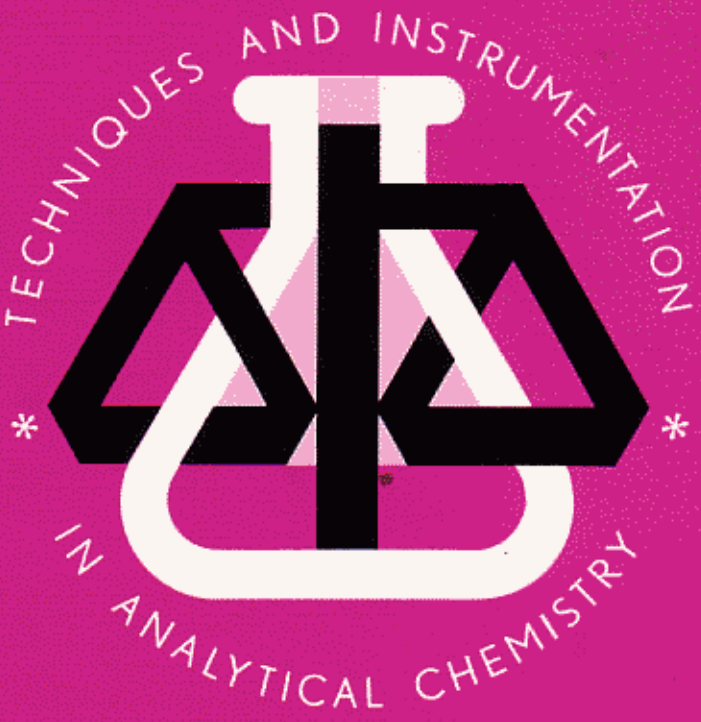

INSTRUMENTAL METHODS IN FOOD ANALYSIS

edited by
J.R.J. Paré and J.M.R. Bélanger

ELSEVIER

TECHNIQUES AND INSTRUMENTATION IN ANALYTICAL CHEMISTRY — VOLUME 18

INSTRUMENTAL METHODS IN FOOD ANALYSIS

Edited by

J.R.J. Paré
J.M.R. Bélanger
Environment Canada, Environmental Technology Centre,
Ottawa, Ontario, Canada K1A OH3

1997
ELSEVIER
Amsterdam — Lausanne — New York — Oxford — Shannon — Tokyo

ELSEVIER SCIENCE B.V.
Sara Burgerhartstraat 25
P.O. Box 211, 1000 AE Amsterdam, The Netherlands

ISBN: 0-444-81868-5

This book is printed on acid-free paper.

Printed in The Netherlands

J.R.J. Paré and J.M.R. Bélanger (Editors)
Instrumental Methods in Food Analysis

Chapter 6

Nuclear Magnetic Resonance Spectroscopy (NMR): Principles and Applications

Calin Deleanu (1) and J. R. Jocelyn Paré (2)

1) "Costin D. Nenitescu" Institute of Organic Chemistry, NMR Department, Spl. Independentei 202 B, P. O. Box 15-258, Bucharest, Romania and 2) Environment Canada, Environmental Technology Centre Ottawa, ON, Canada K1A 0H3

6.1 INTRODUCTION

The Nuclear Magnetic Resonance (NMR) technique is now half a century old [1,2]. One might consider this as a long time, or at least as a time sufficiently long to justify the fact that NMR is by now a technique present in both advanced research and basic undergraduate courses in so many fields like chemistry, physics, biology, food sciences, medicine, material sciences, and so on. But if we consider the formidable progress that took place in these years, with NMR opening several stand-alone research fields (to mention only liquid-, solid-, localized-, low resolution-NMR, NMR Imaging and Microscopy) and the explosion of new techniques and instrumentation, then 50 years is a rather short time. By now, high resolution NMR is the most powerful technique for structure elucidation of chemical compounds in solution. It is also one of the most expensive techniques in terms of equipment, but meanwhile, very significantly, a technique which is already part of almost all research and teaching establishments. While the manufacturers are continuously pushing the limits of the instrumentation, trying to cope with every day developments in theoretical knowledge, the research, teaching and health establishments keep buying equipment costing roughly a million US

dollars each, knowing exactly that the last generation of equipment they just bought will be obsolete in less than 5 years, requiring thus continuous costly upgrading, and probably a new purchase in ten or fifteen years. Moreover, high resolution NMR spectrometers are some of the instruments with the highest running costs. Clearly, there is something very interesting going on around NMR, and those who will not be able to cope with these developments will face a disadvantage in many research fields. But this is only one of the medal's face, namely that of the advanced research. On the other side there are already established NMR analytical techniques for which low cost routine spectrometers have been developed, and where NMR proved in many cases to be the most competitive method in terms of costs, man-power, time, accuracy and in some cases the only acceptable method. The readers of this book should be familiar with the need of solving problems like determining the solid phase content in fats, water content of pulped sugar, total fat content, oil content of seeds, or the geographic origin of wines, for which NMR is a very competitive method and often the best method available to date.

The following part of the present chapter will present an introduction to the NMR field, trying to avoid deep mathematical and physical explanations, but rather presenting the conclusions of these treatments. For those interested in a deeper presentation of various topics which follow, references to more extensive books are made.

6.2 NOTES ON LITERATURE

Clearly, trying to cover a domain so vast as NMR in all its aspects ranging from theory, *via* fundamental research, to established routine analyses is a difficult task even for a dedicated book. We will therefore go through some aspects of the NMR phenomenon and we will recommend some books (among very many NMR books one could find in a library's index guide) dealing with various aspects of the field.

For NMR spectroscopists there is a quasi general consensus in quoting the Bible of the field, with its Old (published in 1959 by Pople, Schneider and Bernstein) [3] and New Testament (by Ernst, Bodenhausen and Wokaun) [4]. Other books, dealing more with the theory of the phenomenon than with its applications, could be recommended [5-9].

Very good introductory books, [10-12] with a pragmatic approach, focusing on structure elucidation, are quoted here rather as a subjective option of the authors, than an attempt to list all the good NMR books. An easy to read book with a very special flavor, which stimulates those who actually want to themselves play with the spectrometer is Derome's book [13]. Books dealing with specialized aspects and applications of NMR to chemistry, biology, biochemistry and medicine are also available. Surprisingly, one would have difficulties in quoting books devoted to NMR in food sciences. We are aware

of only one book devoted exclusively to NMR applied to food sciences [14]. One reason for this might be a wide spread general feeling that NMR is a too expensive technique in comparison with the benefits it generates. A very wrong idea, both in terms of unicity of some of the information provided (one only needs to have a look to the major food science journals publishing NMR papers) and of the existence of specially designed low cost analytical instruments.

Another aspect we would like to underline is the general fact that because of the continuously increasing amount of publications, it becomes more and more difficult to handle the information. Thus, some specialized databases and abstracting publications tend to become the principal guiding source through the literature in some particular fields. The advantages of carrying out an electronic search are obvious, and there is no need to emphasize here this aspect. The drawback however, particularly for NMR, is that these abstracting publications cover almost exclusively journals in fields like chemical, medical, biological, or food sciences, with little cross references. Thus, there is some risk of rediscovering the wheel in terms of NMR applications. If one carries NMR searches for a particular topic in a particular science domain, we strongly advise carrying searches for the same topic in the other mentioned domains.

Thus, looking to the NMR keyword in *Food Sciences and Technology Abstracts*, on CD-ROM, until June 1996, we could find only one book exclusively dedicated to the NMR field [14]. The same search revealed several books specialized in a particular food stuff or covering general analytical techniques, having a chapter in NMR. The present chapter is by no means trying to cover this gap, but only to draw attention to various aspects of NMR in food sciences, literature data being one of these aspects.

6.3 THE ELECTROMAGNETIC SPECTRUM

Similarly to other forms of molecular spectroscopy, the NMR phenomenon is associated with absorption and emission of energy. Before going into the details of NMR it is useful to compare the energy associated with it with the energy required to produce other types of spectroscopy in the context of the continuous electromagnetic spectrum (Figure 1).

An absorption spectrum (Figure 2) is a line, or a collection of lines of various intensities situated at different frequency (or wavelength) positions. These lines in the spectrum correspond to transitions between various energy levels in the studied molecule (Figure 3). The transitions are stimulated by the electromagnetic radiation having exactly the same energy ($E_0 = h\nu_0$) as the energy gap (ΔE) between the affected energy levels.

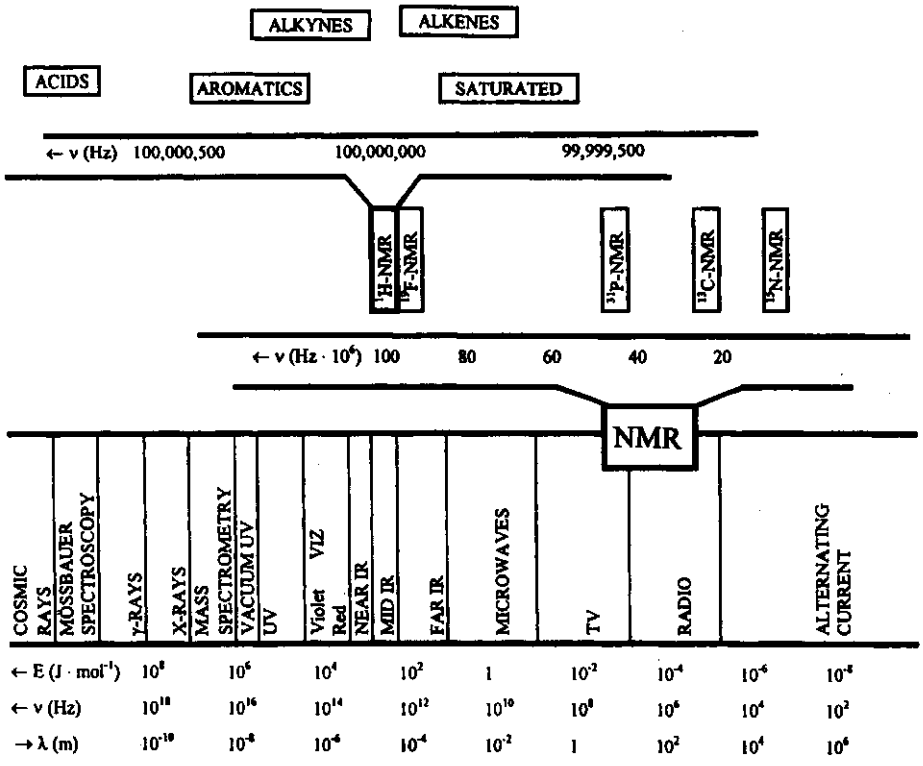

Figure 1: The electromagnetic spectrum.

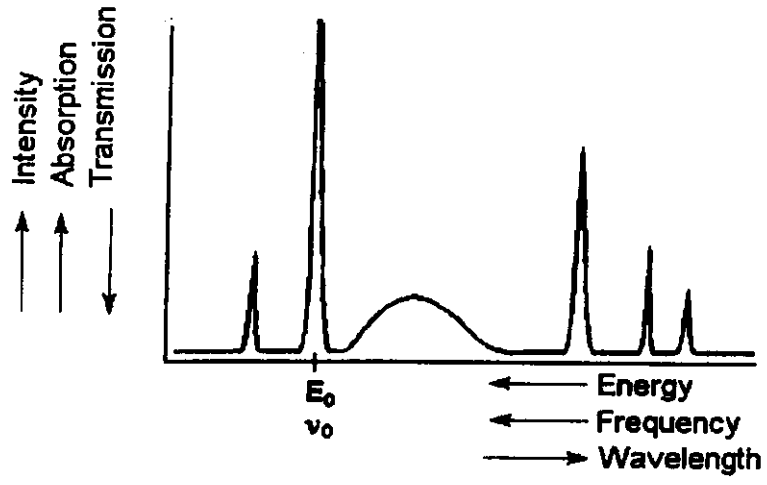

Figure 2: An absorption spectrum and the associated parameters.

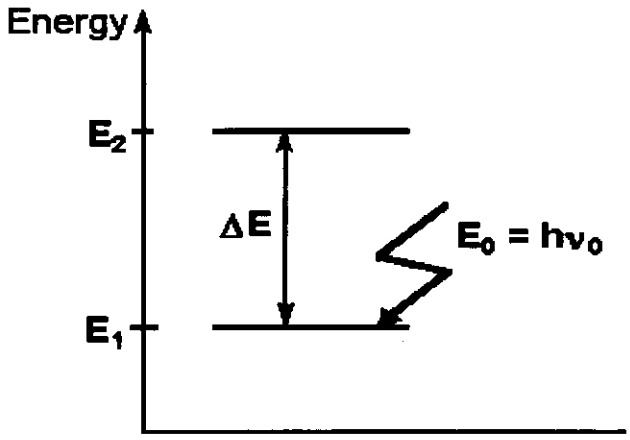

Figure 3: Energy levels in atoms and stimulation of transitions by external energy.

Going back to the electromagnetic spectrum, one can easily note that the energy associated with the NMR phenomenon is very weak in comparison with the other common types of spectroscopy. The radiation generating the NMR transitions is situated in the radiofrequency domain.

The difference between NMR and other forms of spectroscopy is that the absorption of energy takes place only in the presence of a magnetic filed.

6.4 THE NMR PHENOMENON

6.4.1. Nuclei active in NMR

Some atomic nuclei behave like microscopic bar magnets. The general condition for a nucleus to behave in this way is to have an odd number of protons and/or neutrons (*i.e.*, to have the spin quantum number, *I* different from zero). Most common nuclei in NMR (^{1}H, ^{13}C, ^{31}P, ^{19}F) have the spin number (*I*) equal 1/2 and are named *spin 1/2 nuclei*. The following discussion will be particularized for the spin 1/2 nuclei, but the general rules and conclusions are valid for all cases.

Fortunately, although not all the nuclei in the periodic table are active in NMR, almost every element has one or more than one isotope active in NMR. Some difficulties arise when the natural abundance of the active isotopes is very low. But with present instrumentation, spectra of practically any active nucleus can be recorded.

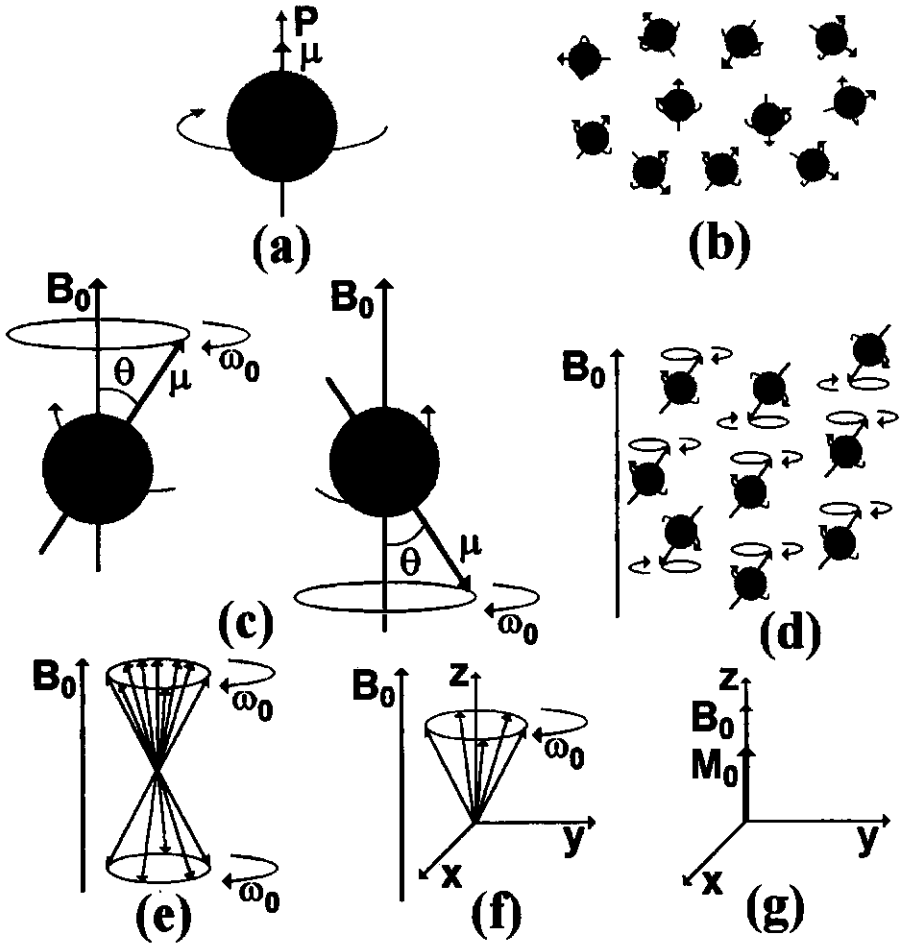

Figure 4: Magnetic properties of nuclei with spin quantum number ½; a) an electrically charged nucleus under the spinning motion generates an angular momentum *P* and a magnetic moment μ; b) in the absence of an external magnetic field the individual magnetic moments are randomly oriented; c) in the presence of an external magnetic field B_0 the spin ½ nuclei may adopt only one of the two allowed orientations; d) under the influence of an external magnetic field all nuclei in the sample adopt one of the allowed orientations; e) the number of nuclei oriented parallel to the external magnetic field is slightly greater than the number of nuclei oriented antiparallel. Only the individual magnetic moments are shown; f) the uncancelled magnetic moments; g) the macroscopic result of the excess magnetic moments is a global magnetization M_o pointing the same direction as the external magnetic field.

6.4.2. Nuclei in an external magnetic field. The equilibrium

An electrically charged body when rotating generates a magnetic field. Obeying to this universal law, the nucleus of an atom being electrically charged, and spinning generates a magnetic field (Figure 4a). Doing this, it behaves like a bar magnet, and is able to interact with other magnetic fields. The generated *magnetic moment* (μ) is proportional to the *angular momentum* (P). The proportionality factor γ is named *gyromagnetic ratio* and is a constant for each nucleus type.

$$\mu = \gamma P$$

In the absence of other magnetic fields, the magnetic moments (μ) for a collection of many atoms are randomly oriented and in continuous reorientation due to thermal motion (Figure 4b). The result is that the macroscopic sample has no magnetization, because of the averaging to zero of the elementary magnetic moments.

If an *external magnetic field* (B_0) is applied to the sample, the magnetic moments are allowed to adopt only some quantized orientations (*e.g.*, θ = 54°44' for ^1H nuclei) in relation with this field (Figure 4c). In this situation a supplementary movement takes place. The magnetic moment (μ) precesses around the direction of the external magnetic field (B_0) with an angular speed ω_0 (*e.g.*, for ^1H nuclei in a field B_0 of 2.35 T, ω_0 is 100 MHz, *i.e.*, 100,000,000 rotations per second). The rotation frequency ω_0 is named the *Larmor frequency* and is in fact the *absorption frequency* of that particular type of nucleus in a certain external magnetic field (B_0). This rotation can be clockwise or counterclockwise, depending on the sign of the gyromagnetic ratio (γ).

$$\omega_0 = - \gamma B_0$$

Thus, in the presence of the external magnetic field B_0 all the individual magnetic moments adopt one of the allowed orientations (Figure 4d). For nuclei spin 1/2, only two orientations are allowed: *"parallel"* (by convention designed as $\uparrow$) and *"antiparallel"* ($\downarrow$) to the external magnetic field. The two allowed orientations have different energies, thus the number of nuclei adopting each orientation is not equal (Figure 4e). The lower energy state (parallel to the B_0 field for the positive γ nuclei) is the most populated one. The macroscopic result of this status is that the individual magnetic moments, do not cancel to zero anymore, but produce a net magnetization (M_0) on the direction of the external magnetic field (z axis) pointing in the same direction as the individual magnetic moments in the more populated orientation (Figure 4f,g). In the equilibrium situation the precessing

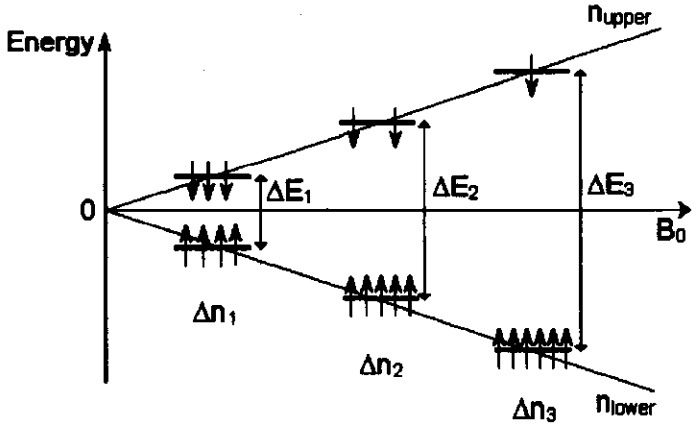

Figure 5: The dependence of the energy gap (ΔE) between parallel and antiparallel orientations of atomic nuclei on the strength of the external magnetic field (B_0) The difference in populations (Δn) also increases as the magnetic field strength increases.

magnetic moments are randomly distributed on the surface of a cone around the z axis, thus their projections in the x-y plane canceling to zero (Figure 4f). The macroscopic result is that there is no net magnetization in the x-y plane, but only along the z axis (Figure 4g).

The energy gap (ΔE) between spatially quantized (allowed) orientations of the magnetic moments (Figure 5) depends on the gyromagnetic ratio (γ, which is a constant for each type of nucleus) and on the external magnetic field applied to the sample (B_0, which is dependent on the strength of the magnet, thus being dependent on the constructive characteristics of the spectrometer).

$$\Delta E = \gamma h B_0 / 2\pi$$

where, h is the Planck's constant.

6.4.3 The Resonance condition

In order to induce the NMR phenomenon, irradiation of the sample with a frequency (ν_0) corresponding to the energy gap between the two energetic levels (parallel and antiparallel in the previous example) should be performed. The energy required ($E_0 = h\nu_0$) is in the radiofrequency range, the associated frequency having values between 10 MHz (or even less) and 800 MHz (the present instrumental limit), depending on the type of instrument and nucleus. It is very common to refer to a particular spectrometer in terms of absorption frequency for the ^1H nuclei rather than in terms magnetic field strength.

TABLE 1
Gyromagnetic Ratios and Resonance Frequencies for Some Common Nuclei at Different Magnetic Flux Densities (B_0)

Isotope	^{1}H	^{13}C	^{31}P	^{19}F	^{15}N
Giromagnetic Ratio, γ (10^7 rad T^{-1} s^{-1})	26.7519	6.7283	10.8394	25.1815	-2.7126
Natural abundance (%)	99.98	1.11	100	100	0.37
Absolute sensitivity*	1.00	$1.8\ 10^{-4}$	$6.6\ 10^{-2}$	0.83	$3.9\ 10^{-6}$
Magnetic Field (T)	Resonance frequency (MHz)				
0.23	10	2.5	4.1	9.4	1.0
0.47	20	5.0	8.1	18.8	2.0
1.41	60	15.1	24.3	56.5	6.1
1.88	80	20.1	32.4	75.3	8.1
2.11	90	22.6	36.5	84.7	9.1
2.35	100	25.1	40.5	94.1	10.1
4.70	200	50.3	81.0	188.2	20.3
5.87	250	62.9	101.2	235.2	25.3
7.05	300	75.4	121.4	282.2	30.4
9.40	400	100.6	161.9	376.3	40.5
11.74	500	125.7	202.4	470.4	50.7
14.09	600	150.9	242.9	564.5	60.8
17.62	750	188.6	303.6	705.6	76.0

*This is the sensitivity at constant field, taking into account the natural abundance.

The absorption of energy stimulating transitions between the two levels of energy in a magnetic field is called *magnetic resonance*. Thus, the *resonance condition* obtained by equaling E_0 to ΔE can be expressed either as:

$$\nu_0 = \gamma B_0 / 2\pi$$

or (using the angular frequency $\omega_0 = 2\pi\nu_0$), as:

$$\omega_0 = \gamma B_0$$

Table 1 presents gyromagnetic ratios and resonance frequencies for some common nuclei at different magnetic flux densities (B_0).

6.4.4. Inducing a population inversion

One can imagine two ways to invert the populations of the two energetic states (n_{lower} and n_{upper}). One way would be to invert the direction of the B_0

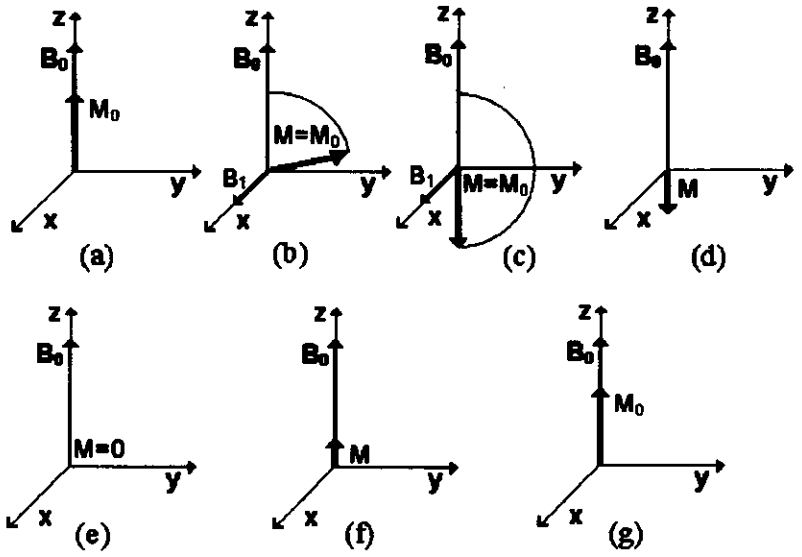

Figure 6: A simplified description of the evolution of the magnetization during an NMR experiment. In reality this evolution is characteristic for the projection of the magnetization vector M on the z axis M_z. a) the equilibrium; b) and c) the effect of a perpendicularly magnetic field B_1; d) to g) relaxation.

field for a while, than to suddenly come back to the initial orientation. The other way could be to apply another magnetic field (B_1) pointing along the x axis for a while. This second possibility is in fact the experimental solution.

The effect of a perpendicularly oriented field (B_1) is to rotate the magnetization around it in the y-z plane (Figure 6b,c). Depending on how this secondary magnetic field is applied, there are two fundamentally different types of spectrometers, namely: *Continuous Wave* (CW) and *Pulse Fourier Transform* (PFT) spectrometers. In the CW case the magnetic field B_1 (with its associated frequency ν_1) is continuously increased from the beginning of the experiment until its end. In this way, when the resonance condition is reached for a particular type of nuclei, (thus ν_1 becoming equal with ν_0), the energy is absorbed, transitions take place and the magnetization M_0 deviates (as in Figure 6b). As the B_1 field further increases, the energy is no longer absorbed, and the populations return to the initial states, the magnetization (M_0) returning also to its initial position (Figure 6a). As the continuously increasing B_1 field matches the resonance condition for another type of nuclei in the sample (ν_{02}), energy is again absorbed, magnetization flips and a new signal is recorded by the spectrometer. It is important to note that signals for a sample are acquired one by one as the monochromatic CW

frequency associated with the field B_1 exactly matches the resonance frequency for each particular type of nuclei. The sweeping of the whole range of frequencies usually takes a few minutes. As this type of spectrometers are less and less used because of many inconveniences, the description of the CW technique has only a theoretical and historical importance. All the remaining of the discussion will refer exclusively to the PFT technique. The same effect of flipping the magnetization (M_0) around the x axis is achieved in PFT NMR spectroscopy, by applying for a very short time (in the range of microseconds) an intense pulse of polychromatic frequencies, thus the B_1 field matching the resonance conditions for a much broader range of nuclei. Usually all the nuclei of a particular element in the sample (regardless of their environment in the molecule) are turned around the *x* axis (Figure 6b) during the radiofrequency (r.f.) pulse. It takes only a few microseconds to accomplish the resonance condition for a whole range of nuclei, and then (*i.e.*, after the magnetization M_0 has been inverted), the r.f. pulse is turned off.

6.4.5. Returning to the equilibrium. Relaxation

Once the temporary magnetic field B_1 (which, for reasons not developed in our simplified treatment, is an oscillating field) is turned off, the system which was perturbed returns to normal. The process of returning to the equilibrium status is called *relaxation*. We recall that the macroscopic magnetization is in fact the vectorial resultant of the individual magnetic moments precessing around the B_0 field (*i.e.*, z axis). Thus, as the population returns to normal, less and less nuclei are in the upper energy state, until they reach the initial difference Δn for the equilibrium state. This process should have as effect an evolution of the macroscopic magnetization as in Figure 6d-g. In reality this is what is happening with the projection of the magnetization (M) on the *z* axis (M_z). As it regards the global magnetization vector, this vector once flipped away from the z axis (Figure 6b) is subjected to the same tendency as the individual magnetic moments μ (Figure 4c-f), thus rotating around the z axis (*i.e.*, B_0 field) (Figure 7a). The magnetization M_0 is subjected to two tendencies. One tendency is to rotate (precess) around the B_0 field (Figure 7a), the other tendency is to flip back to the position parallel with the z axis, pointing the same direction as the B_0 field (positive z axis) (Figure 4.4b). The result of these two tendencies simultaneously acting on the magnetization is a recovery trajectory as in Figure 7c. During the relaxation process, one can imagine the arrow of the magnetization vector always touching the internal surface of a sphere.

6.4.6. The NMR signal. Free Induction Decay

The trajectory of the magnetization after the r.f. pulse is shown in Figure 7c. As the magnetization turns around the z axis the projection on the y axis evolves between a maximum positive and a minimum negative value (Figure 7d). The reason why the maxima and minims have not always the same

magnitude, is that each time the magnetization crosses the y-z plane it does it under a different flip angle (α), *i.e.*, the arrow of the magnetization vector touches another x-y plane of the sphere it describes. The evolution of the projection of the magnetization on the z axis as a function of time is easier to understand. Thus, as the flip angle goes smaller, the projection returns toward the initial M_0 value, and doing this it passes through the zero value (Figure 7e). The free evolution of the magnetization after an r.f. pulse is called *Free Induction Decay* (FID). The recorded FID (detected as a projection of the magnetization on the y axis) is in fact the raw result of an NMR experiment. Usually the NMR experiment ends up with a so called detection pulse which turns the magnetization M_0 by a *flip angle* (α) of 90° or smaller. Thus the evolution of the magnetization in time during the detection of the FID reassembles the Figures 4.4f-h, the most common pattern for the FID being that in Figure 7g.

Although the NMR experiment is considered finished once the signal (FID) was recorded and the detector was switched off, the resulted signal is of limited help for the analyst because of its complexity. In order to obtain the NMR spectrum one should transform the time domain data into a frequency domain data. Figure 8 shows the forms of the two functions we just mentioned, namely f_2 which represents the amplitude of the signal as a function of time (Figure 8a), actually the FID, and f_1 which represents the amplitude of the signal as a function of frequency (Figure 8b), actually the NMR spectrum. The mathematical transformation linking these two functions is called *Fourier transform* (FT):

$$f_1(\omega) = \int_{-\infty}^{+\infty} f_2(t)\, e^{-\omega t}\, dt$$

For a real signal resulting from a sample containing more than one kind of nuclei, thus presenting more than one line in the NMR spectrum, the actual FID is much more complex than that shown in Figure 8a In fact the complexity of the FID was the principal factor delaying the introduction of FT-NMR spectrometers and pulse techniques until the 1970s. Nowadays we do not have to bother anymore with the transformation itself, as this is automatically performed by the spectrometer's computer. However there are other treatments of the FID signal previous to its Fourier transformation of which the spectroscopist should be aware. On the way the signal is processed depend very important characteristics of the NMR spectrum, like the resolution or sensitivity. Last but not least, we should mention that FT is by far the most popular way of transforming the FID into the frequency spectrum, but it is not the only way.

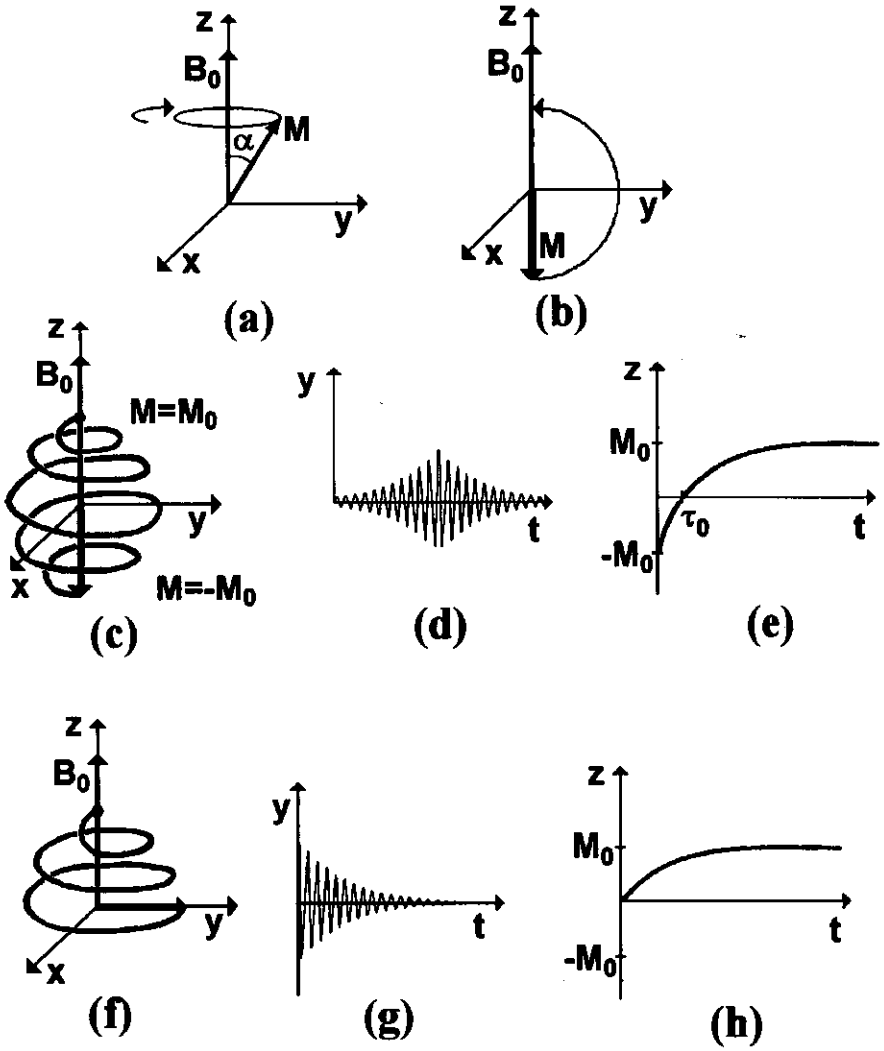

Figure 7: A more accurate description of the relaxation process: a) one of the tendencies of a tipped magnetization is to precess around the external magnetic field; b) another tendency is to realign parallel with the external magnetic field; c) the actual trajectory of the magnetization under the combination of the two tendencies after a 180° pulse; d) projection of the magnetization on the y axis after a 180° pulse; e) projection of the evolution of the magnetization on the z axis after a 180° pulse; f) the trajectory of the magnetization during relaxation after a 90° pulse; g) projection of the magnetization on the y axis after a 90° pulse; h) projection of the evolution of the magnetization on the z axis after a 90° pulse.

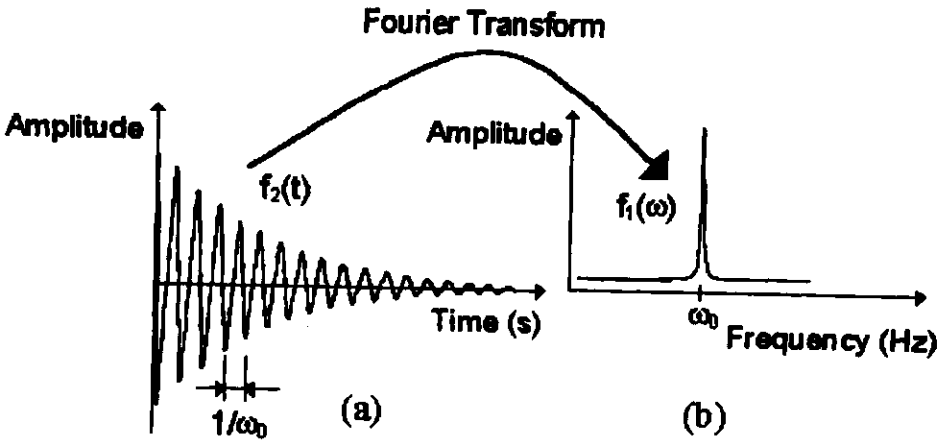

Figure 8: The two forms of the NMR data; a) the FID representing the signal as a function of time and b) the spectrum representing the signal as a function of frequency.

6.5. TYPES OF INFORMATION PROVIDED BY THE NMR SPECTRA

6.5.1 Chemical Shifts

The nucleus of a particular element which is part of a molecule experiences an effective magnetic field (B_{ef}) which is smaller than the external magnetic field B_0. The reason for this phenomenon is the shielding of the nucleus by electrons. The electrons shielding the nucleus could be those belonging to the same atom, those involving the atom in chemical bonds or those of the neighbor atoms. Each atom (of the same element) in a different position in a molecule will have a different electronic surrounding, thus experiencing a different effective magnetic field. The difference between the resonance frequency of a free nucleus and the same nucleus in a chemical environment is named *chemical shift*. The chemical shift is measured by the dimensionless parameter δ as the difference between the resonance frequency of the studied nucleus (ν) and the resonance frequency of the nucleus of the same element in a reference compound (ν_{ref}). In order to make this parameter independent of the field strength (and thus independent of the constructive characteristics of the spectrometer) the difference frequency is also divided to the resonance frequency of the standard. As the difference in frequency is very small, the resulting expression is further multiplied with 10^6, thus the chemical shift δ being expressed as parts per million (ppm):

$$\delta = [(\nu - \nu_{ref})/\nu_{ref}]\ 10^6$$

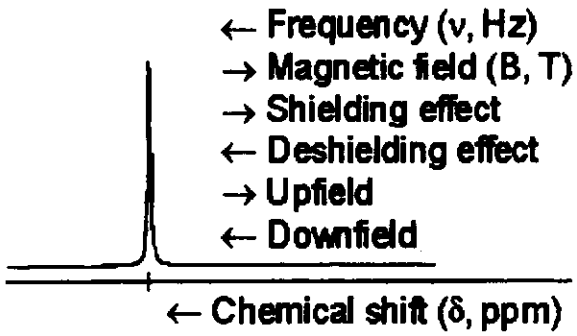

Figure 9: Parameters and nomenclature associated with the NMR spectrum.

The most usual reference standard is the tetramethylsilane (TMS) which is used for both ^{1}H- and ^{13}C-nuclei in organic solvents. For aqueous solutions other standards like sodium 3-trimethylsilylpropionate or dioxane are used. When referring to an NMR spectrum the conventions as in Figure 9. are used. Note that the scale under the spectrum should always be marked in δ values.

6.5.2. Intensity of the signals

The area under a NMR signal is proportional to the number of nuclei giving rise to that signal. Thus the ratios of the integrals of various signals in the NMR spectrum represent the relative numbers of atoms for those signals. This property is very valuable in structure elucidation problems. If one refers the integrals of signals in a sample, to the integral of a signal belonging to a compound which was added in a known concentration to the sample, then the concentrations of compounds in complex mixtures can be determined. The accuracy of the integration of NMR signals depends dramatically on the experimental conditions. Each type of nucleus has different characteristics in terms of relaxation properties. In order to obtain fully relaxed signals, one should employ appropriate waiting (relaxation) delays.

Another aspect of the problem is the sensitivity of the spectrum. This is commonly expressed as the signal-to-noise ratio. There are many aspects influencing the sensitivity, among them the gyromagnetic ratio and the natural abundance are the most important ones.

The external magnetic field (B_0) also influences the sensitivity. The dependence of the energy gap (ΔE) on the strength of the external magnetic field (B_0) was presented in Figure 5. It is important to note that as the B_0 field increases it is not only the energy gap that increases, but as a

consequence of this, the population difference Δn between the lower and upper energy levels that also increases.

$$\Delta n = n_{lower} - n_{upper}$$

The immediate result of this observation is that, for instance when a transition of the type ΔE_3 is induced, in comparison with a ΔE_2 transition (Figure 5), the intensity of the corresponding line in the spectrum would be higher. Thus, one of the advantages of recording NMR spectra at the highest available magnetic field is the increase in sensitivity.

There are other ways to increase the intensity of the signal, but on compromising on the accuracy of the quantitation (see section 6.5.6).

6.5.3 Coupling Constants. Spin-spin coupling

As each individual nucleus active in NMR behaves as a small magnet it is not surprising that these local magnetic fields interact for neighboring nuclei in a molecule. There are several ways in which the magnetic nuclei interact. We will focus now on the interactions of nuclei through chemical bonds. Although we will not try to provide a detailed explanation for this, it is essential to remember that this sort of interaction is mediated by the bonding electrons. Thus, the most intense effect is to be expected for nuclei directly bonded, and the effect is expected to diminish as the number of bonds between two nuclei increases. As we find it logical to expect an interaction between connected magnetic nuclei, we should see now which is the effect of this interaction in the NMR spectrum. The observable effect is the splitting of the signal of a particular nucleus in direct relationship with the number and type of neighboring nuclei. As the vast majority of organic compounds contain hydrogen atoms, and as the natural abundance of the magnetic active isotope ^1H is very high (Table 1), it is to be expected that most of the compounds we are encountering will have spectra with patterns complicated by these splittings. In fact the coupling patterns provide very valuable information for structure assignments. In some cases however (*e.g.*, when observing ^{13}C-nuclei) it is useful to remove this interaction (using the decoupling technique) and obtain single peaks for each type of nucleus. Even in these cases the coupling constants are of tremendous importance. There are a huge number of possibilities for exploiting the coupling effects in both one and multidimensional NMR spectra. Recording most of the spectra mentioned in *section* 6.5.9 is possible only by playing with the through-bond coupling effects. Figure 10 provides an explanation for the coupling patterns.

As it was shown previously (Figure 9) the strength of the magnetic field is increasing in a NMR spectrum from left to right. If we consider two magnetically active nuclei (*e.g.*, protons) belonging to the same molecule, but situated at a distance sufficiently big so that the effect of their local magnetic

fields is not transmitted through bonds, than the signals of these nuclei (H^A and H^B) are singlets positioned in the spectrum according only to the influence of the chemical shift (Figure 10a). We recall that the effective magnetic field experienced by a particular nucleus (*e.g.*, H^A) depends on the strength of the shielding effect of the surrounding electrons. In the same way (if the through-bond distance is short), another local magnetic field (*e.g.*, generated by H^B) could alter the effective magnetic field experienced by the observed nucleus (H^A). The difference in this case is that the local magnetic field could have two directions (for nuclei with spin quantum number higher than 1/2, more than two directions are allowed). Thus, half (almost half, with a very good approximation) of the population of the neighbor nuclei (H^B) are producing a local field at the position of the observed nuclei (H^A) which is parallel (↑) with the external field (B_0), and the other half of nuclei H^B are producing a local field of the same magnitude but opposing the external field (↓) (Figure 10b). The effect of these two additional magnetic fields is that for half of the population of the observed nuclei (H^A) the effective magnetic field is increased (↑) and for the other half the effective magnetic field is diminished (↓). Thus, in one case (↑) the required external magnetic field for the resonance of H^A is smaller because it is "helped" by the added magnetic field produced by H^B, whereas for the other case (↓) the external magnetic field required to produce the resonance of the same nuclei H^A is bigger because it has to overcome the "opposition" of the additional magnetic field produced by H^B. The result in the spectrum is that instead of one line corresponding to the resonance position of the H^A nuclei, there are two equally intense lines, *i.e.*, a doublet pattern (Figure 10b). The same effect has the proton H^A on the signal of the proton H^B. Thus the difference between the two lines of the H^A doublet (denoted J_{AB}) is equal with the distance between the lines of the H^B doublet (J_{BA}).

Figure 10c presents the splitting pattern of the observed proton (H^A) in the presence of two identical neighboring protons (H^B). A similar judgment allows us to draw all possible combinations for the two additional magnetic fields produced by two protons H^B at the position of the proton H^A. Thus, when both H^B protons are producing a field which adds to the external magnetic field (↑↑), the signal in the spectrum appears deshielded, on the contrary, when the field generated by the both H^B protons opposes the external magnetic field, the signal in the spectrum is shielded. There is also the possibility that one of the H^B protons generates a parallel and the other an antiparallel local field (↑↓). In this case the two fields cancel each other and the external magnetic field is not affected. The signal in the spectrum appears at the position dictated only by the chemical shift of the H^A proton. There is also still another possible combination, namely when the first considered H^B proton generates an antiparallel field and the second one a parallel oriented magnetic field (↓↑). Of course, one cannot distinguish between the last two combinations (↑↓ and ↓↑), the lines in the spectrum

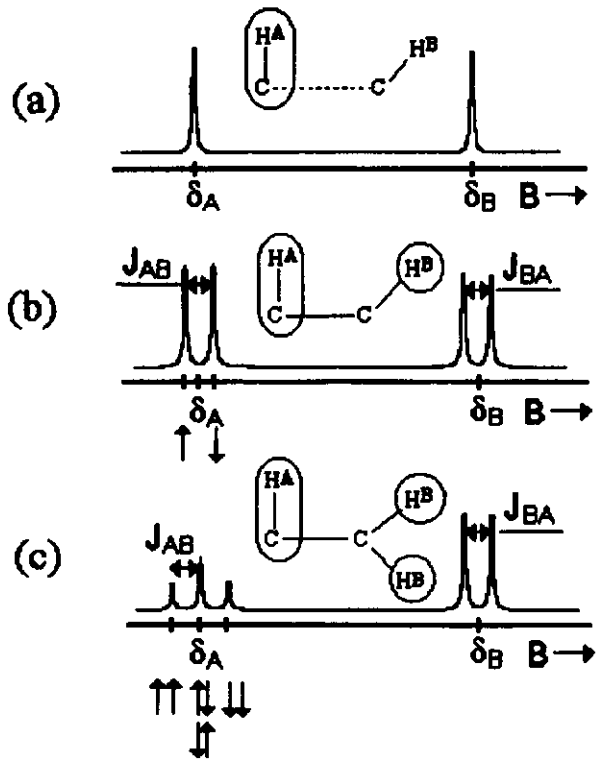

Figure 10: The effect of spin-spin coupling on the NMR spectrum of two hydrogen atoms H^A and H^B ; a) if the number of chemical bonds separating the two atoms is sufficiently great, there is no observable coupling effect; b) two atoms separated by a small number of bonds show characteristic doublet coupling patterns; c) an atom (H^A) having two equivalent neighbor atoms (H^B) shows a characteristic triplet coupling pattern.

appearing in the same place. However, as the two degenerate combinations arise from a population of H^B nuclei which is double than in the first two cases, the inner line of the triplet has a double intensity in comparison with either of the outer lines. In the same way it can be predicted the pattern of a signal under the influence of regardless how many neighboring magnetic nuclei. If the neighboring nuclei are not identical, then the pattern is more complicated.

In all cases the chemical shift of the H^A nuclei is unaltered, thus is situated in the middle of the doublet in the first case or on the position of the central line of the triplet in the second case. The distance between the two lines is called *coupling constant* (J) and it is always expressed in Hz, as it is not affected by

the strength of the external magnetic field (it is independent of the type of spectrometer). We recall that the chemical shift is never expressed in Hz (because in this way it would be field dependent), but in the dimensionless parameter δ as ppm (which is field independent).

It is easy to accept now that the strength of the coupling constant depends on the strength of the local magnetic field produced by the neighboring nuclei. Thus, the coupling constant J will be higher (the distance J_{AB} will be larger) when the neighboring nuclei are closer (less chemical bonds separating them). Also, for the same number and type of bonds the coupling constant J will have different values depending on the geometry of the compound, *i.e.*, the molecular angles. A typical dependence of the coupling constant on the dihedral angle for bonds of the type H-C-C-H is presented in Figure 11.

The equation matching the curve of the coupling constant (J) as a function of the dihedral angle H-C-C-H (φ) is known as the Karplus equation [15]. The original equation predicts very well the coupling constants in saturated compounds. In order to increase the prediction power, several alternatives have been introduced for specific classes of compounds.

The coupling mechanism we discussed in this section is known under the following alternative names: *Spin-spin coupling, Scalar coupling, J-coupling, or Indirect coupling.*

6.5.4. Linewidth of the NMR signal

In order to fully characterize a signal in a NMR spectrum one should list its position (chemical shift), multiplicity (splitting pattern), coupling constant (J) and its linewidth at half-height ($\Delta\nu_{1/2}$).

Figure 12a shows how the half-height linewidth is measured. For small molecules in solution, typical half-height linewidths are about 0.1 Hz. However, the linewidth depends of several factors which we only mention here. Some of them will be discussed later (sections 6.5.8 and 6.6.2). Thus, the linewidth could be influenced by factors like: relaxation time (short relaxation times like in solids give rise to broad lines whereas, long relaxation times like in liquids give rise to narrow lines, see Figure 12b,c.), the relaxation mechanism (*e.g.*, nuclei with quantum number greater than 1/2 give rise to rather broad lines), chemical exchange, intramolecular rotations, temperature, presence of paramagnetic impurities, the homogeneity of the sample, the homogeneity of the spectrometer's magnetic field, interactions with neighboring nuclei (especially those with spin greater than 1, *e.g.*, ^{14}N), mathematical manipulations of the data prior to the Fourier transformation of the FID (*e.g.*, sensitivity *versus* resolution enhancement), acquisition time, or the number of collected data points. We will not address these problems in this chapter. The interested reader is advised to refer to other books [3-13].

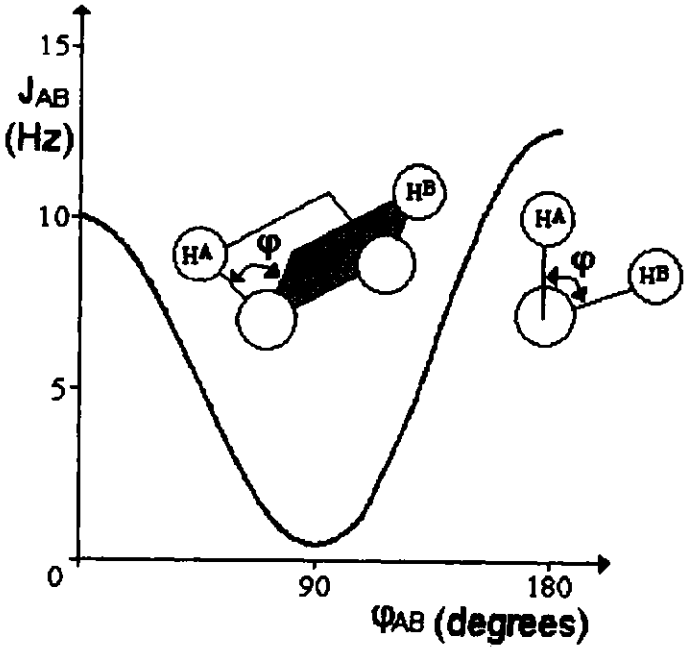

Figure 11: Typical dependence of the three bonds coupling constant J_{AB} on the dihedral angle φ_{AB}.

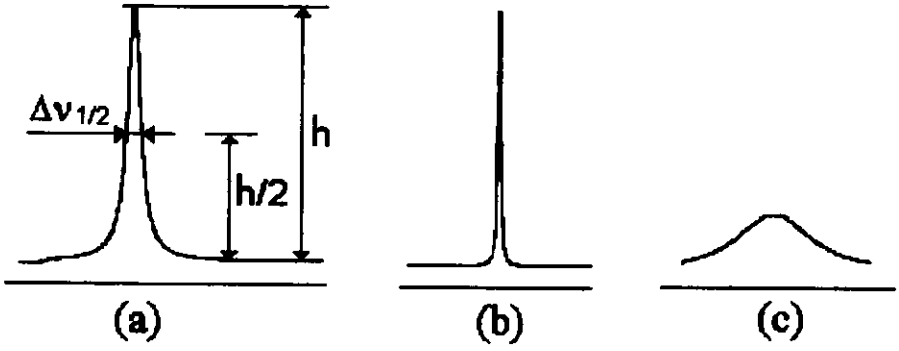

Figure 12: a) Measurement of the half-height linewidth parameter ($\Delta\upsilon_{1/2}$). Small linewidths b) are characteristic for long T_2 relaxation times as in liquids, whereas large linewidths c) are typical for short relaxation times as in solids.

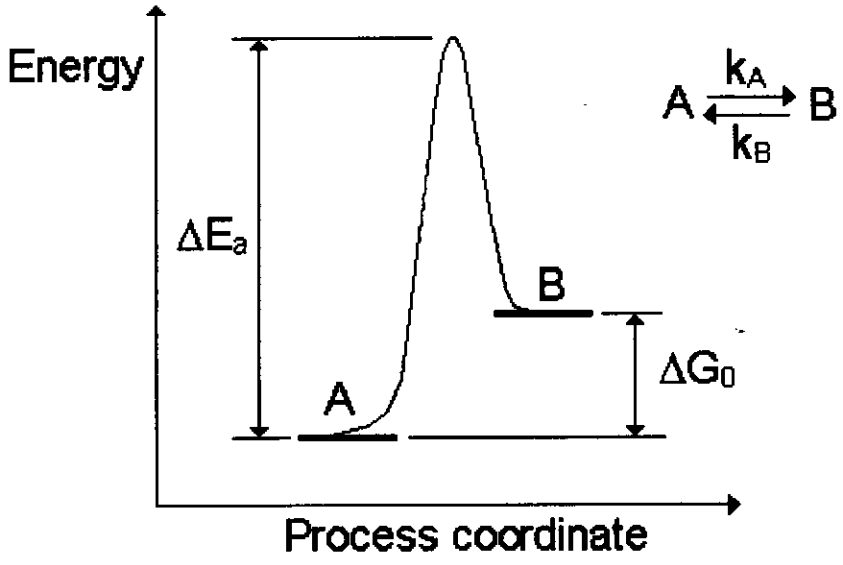

Figure 13: An equilibrium reaction and the associated parameters.

6.5.5 Activation Energies - Chemical Exchange - Dynamic Phenomena

In cases when dynamic equilibria are present NMR can also provide valuable information. An equilibrium of two conformations (A and B) and the associated parameters is presented in Figure 13.

In order to obtain relevant information on the dynamic process, spectra at variable temperature should be recorded. This means that one should record a series of spectra for the same sample at various temperatures ranging from a temperature below the point where the equilibrium is frozen and up to a point where the equilibrium is sufficiently fast that in the NMR spectrum there is no more possible to distinguish the individual signals for the two conformations A and B, but only an average signal. The analysis of this series of spectra takes into account the concentrations of the two species A and B, the temperature where the signals for a particular atom in the two conformations averages (the coalescence temperature), the difference in chemical shifts between the signals of the same atom in the two conformations at low temperature, the half-height linewidths at low temperature, and the signal's multiplicity (splitting pattern). For complex signals it is common to make use of specialized computer programs for lineshape analysis. The information which can be obtained includes: the rate constants (k), the activation energy (E_a), the pre-exponential factor in the Arrhenius function (A) and the difference between free enthalpies of the two conformers (ΔG_0). When more than one mechanism for rearrangements or

other chemical exchange processes are suspected, the variable temperature experiments could also provide valuable information for assigning the pathway of the rearrangement. The same sort of information can be obtained for chemical reactions (*e.g.*, protonation - deprotonation processes). For more details on dynamic NMR we recommend some specialized books [16-18].

6.5.6. Intramolecular Distances. Nuclear Overhauser Effect. Dipolar coupling

Another important property of the magnetic active nuclei is their interaction through space. These interactions take place through different mechanisms than those mediated by the bonding electrons (see section 6.5.3). As in the case of the through bonds spin-spin coupling (responsible for the splitting patterns) the through-space dipolar coupling is also an effect of the local magnetic field generated by the neighboring magnetic nuclei at the position of the observed nucleus.

There is a fundamental difference between the two types of coupling mechanisms. For the spin-spin coupling, the effect of the neighboring nuclei is independent on the orientation of the molecule in the sample (thus, isotropic with respect to the direction of the external magnetic field). For the dipolar interactions (Figure 14) the intensity and direction of the additional field experienced by the observed nucleus (*e.g.*, A) depend on the position of the neighboring nuclei (*e.g.*, B), thus on the relative orientation of the molecule with respect to the external magnetic field (B_0). For instance, in Figure 14a the local field opposes the external field, whereas in the situation described by Figure14b, it adds to it. Note that r is the through-space distance between the two atoms which do not need to be directly bonded. There are two extreme cases, namely the rapid tumbling of small molecules in non viscous solutions, when the effect of dipolar coupling averages to zero, and the solids for which characteristic broad coupling patterns can be seen (see section 6.5.8). In solution, although the splitting pattern of the dipolar coupling cannot be seen, there is another phenomenon which can be observed, namely the *Nuclear Overhauser Effect* (NOE). This effect represents the enhancement (or generally the change in intensity) of the line corresponding to the observed nucleus (A) when a neighboring (in space) nucleus (B) is irradiated.

The normal process for energy dissipation is by interaction with neighboring magnetic nuclei which could absorb the energy of the excited nuclei. These nuclei could be either nuclei belonging to the same molecule or to other molecules (*e.g.*, the solvent). Without trying to explain the mechanism we will only state that the two nuclei (A and B) have a dipolar interaction. Through this dipolar interaction the magnetization of the saturated (irradiated) nucleus B is transferred to the observed nucleus A. In this situation apart from the normal relaxation pathway of the nuclei A (see

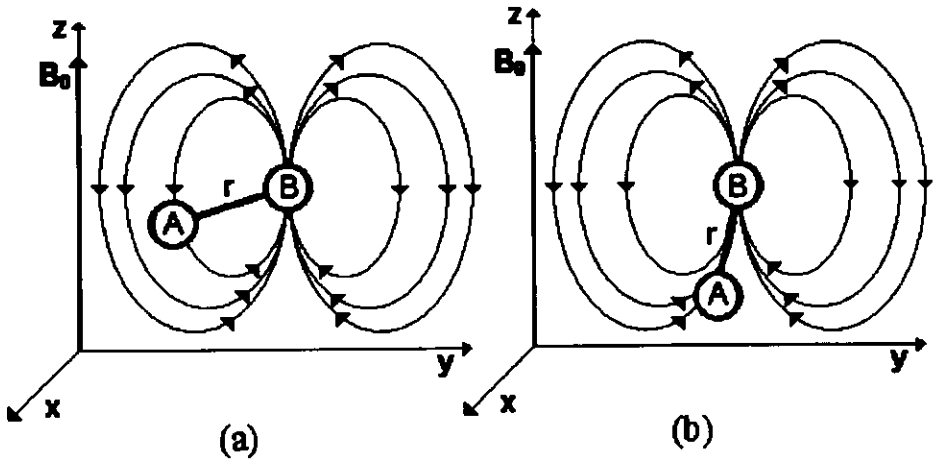

Figure 14: Dipolar coupling. The local magnetic field generated by a neighbor magnetic nucleus (H^B) has different values and orientations at the position of the observed nucleus (H^A) depending on the orientation of the molecule. Thus, in some cases the local field opposes (a) the external magnetic field B_o, whereas in other cases it adds to it (b).

section 6.6.1), another pathway named cross relaxation is available for them (only if the neighboring nucleus B is irradiated). This pathway is made possible by the tumbling motion of the molecule combined with the dipolar interaction, combination leading to a correlated fluctuating local field experienced by both A and B nuclei, the final result being that the two neighboring nuclei can undergo simultaneous reorientation of their spins (spin-flip). The theory is however much more complicated, and we recommend specialized books [19] for those interested.

It is important to underline that the intensity of the lines in the NMR spectrum can be altered by irradiating the neighboring nuclei (Figure 15) and that this through-space effect has very useful applications in assigning the three dimensional structure of molecules. There are several types of spectra which make use of this remarkable phenomenon. For proteins for instance, the assignment of three-dimensional structure in solution is always based on the study of the NOE effects using various types of 2D-, 3D- or 4D-NMR spectra. The change in signal intensity by NOE can be expressed in a quantitative form in terms of efficiency (η_{NOE}), taking into account the original (i_0) and the NOE affected (i) intensities of the observed signal:

$$\eta_{NOE} = (i - i_0) / i_0$$

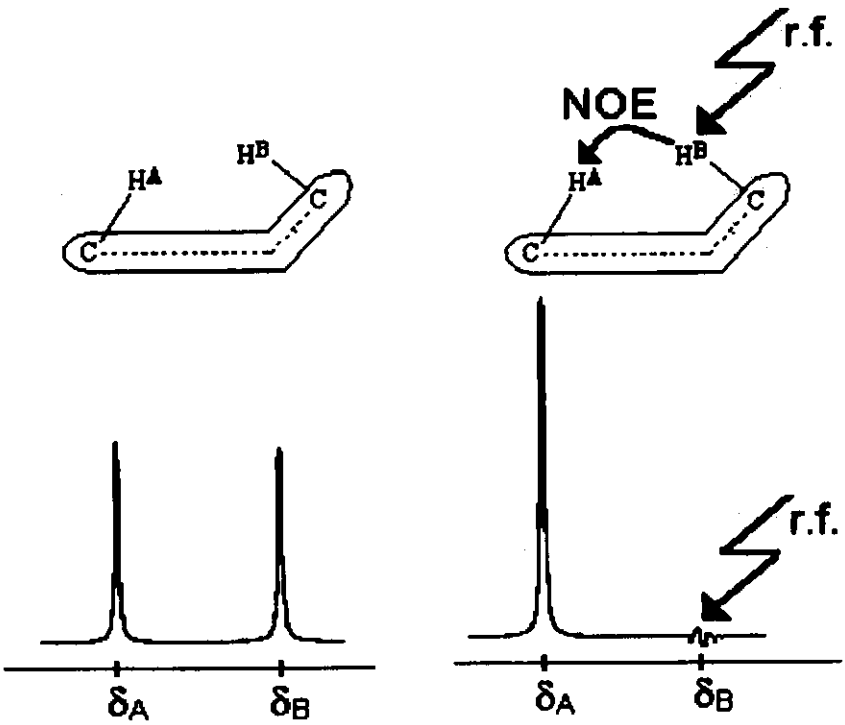

Figure 15: The NOE effect for two neighbor protons; a) in the normal ^{1}H-NMR spectrum the two signals are equally intense; b) When the neighbor H^B proton is irradiated, the intensity of the signal corresponding to the H^A proton is enhanced by the NOE effect.

Finally we should mention that in some cases the NOE effects are unwanted, for instance when exact quantitation is required. In such cases, special experimental measures should be taken, on one hand to minimize the induced NOE and on the other hand to allow sufficient time for any residual NOE to vanish before collecting a new set of data..

6.5.7. Molecular motions

Apart from molecular tumbling (when molecules as a whole undergo translations, rotations and collisions with other molecules under the thermal motion), there are also rotations of atoms and groups of atoms which are intramolecular processes characterizing the structural and energetic states of the studied compound. The NMR techniques could provide valuable information on these processes as well. When the energy associated with these geometrical changes is sufficiently high, energy barriers can be deduced from dynamic NMR spectroscopy as it was mentioned above (section 6.5.5).

Another type of information is provided by the relaxation time associated with each signal in the spectrum. As it was mentioned above (section 6.4.5), the global relaxation time is the time required by a particular atom to return to the equilibrium status (population distribution) after it was excited by an r.f. field. The relaxation time depends (among other factors) on the existence in the neighborhood of the excited nuclei of other magnetic nuclei which could "help" the excited ones to relax faster. Assuming there are some neighboring magnetic nuclei, (*e.g.*, when observing a ^{13}C nucleus which has attached ^{1}H nuclei), there is still another factor affecting the relaxation process, namely the mobility of that part of the molecule. In order to quantify the mobility, the parameter named *correlation time* (τ_C) is commonly used. Correlation time represents the time that a particular site (atom) in the molecule remains in the same position. When a particular atom stays a longer time in a favorable position, the relaxation process is faster. Thus, for small molecules in non-viscous solutions, the relaxation time is shorter for sites with long correlation times. This information is of vital importance for understanding the mobility of various compounds or parts of compounds, *e.g.*, protein chains in various environments or attached to various binding sites.

A good example is a fatty alcohol like decanol [20-22] (Figure 16). In this case owing to the hydrogen bondings which link the OH group to other molecules, the mobility of that side of the molecule is restricted in comparison with the rest of the chain. Thus, the shortest relaxation time (0.65 s) is that of the carbon atom directly linked to the OH group, and the relaxation time increases toward the "free" end of the chain with the CH_3 group having the longest relaxation time (3.10 s). The deduced correlation times from this experimental data show that the shortest correlation time, thus the highest mobility in the chain is experienced by the CH_3 group. If one compares different molecules, it is easy to understand that the small molecules move faster than the large molecules, and also that less viscous solutions allow a faster movement for comparable size molecules. In this way valuable information related to the size of the studied molecule as well as on the medium can be deduced from the correlation time obtained by NMR techniques. Further examples can be found in other books [19, 20]. It is also common to measure relaxation times for broad (unresolved) signals arising from a group of atoms in macromolecules and to deduce mobility information for parts of the molecule on the basis of these "group" relaxation times. Moreover, relaxation times for the whole sample (as in low-resolution NMR), provide very useful information on the physical structure of the sample (Figure 17).

In order to obtain accurate relaxation times, and thus correlation times, special experimental conditions (not so critical for other types of NMR information) have to be ensured. Thus, apart from particular NMR techniques (pulse sequences) one should ensure special sample preparations (*e.g.*, to use appropriate solvents, eliminate any paramagnetic impurity, degas

τ_c (ps/rad)	5	11	15	21	28	28	28	30	30	36
T_1 (s)	3.10	2.20	1.60	1.10	0.84	0.84	0.84	0.77	0.77	0.65

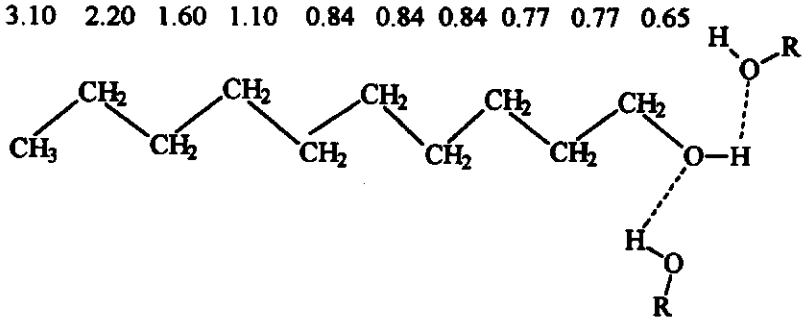

Figure 16: Correlation times (τ_c) and relaxation times (T_1) for carbon atoms in decanol.

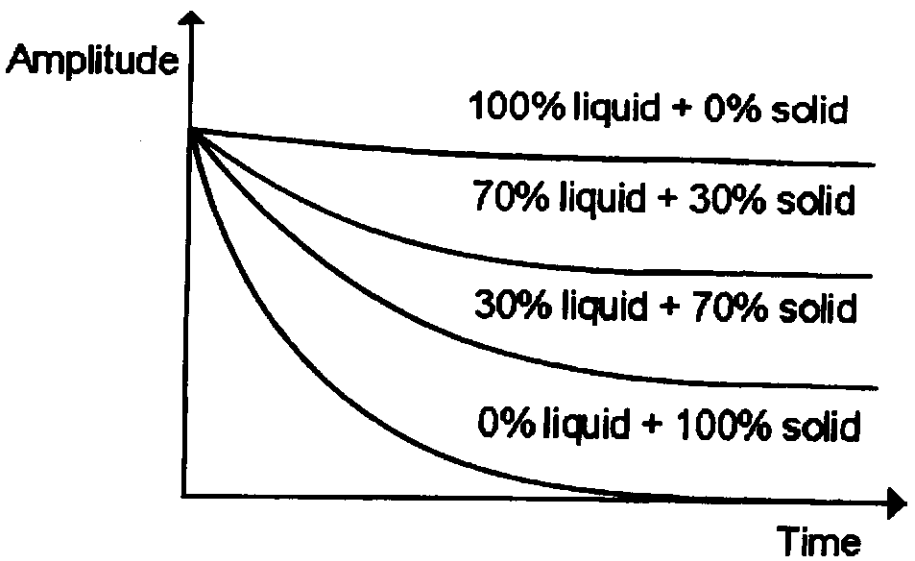

Figure 17: Bulk signal amplitude for samples containing various liquid to solid ratios. The signal decays exponentially with a T_2 relaxation time constant.

the sample). On the other hand, depending on the correlation times for a particular class of compounds, for solving other sorts of problems, and for collecting other types of NMR information as discussed in previous sections, the experimental conditions for recording NMR spectra have to be adjusted accordingly (*e.g.*, to employ appropriate relaxation delays, adjust the viscosity of the solvent, intentionally add paramagnetic compounds to the sample).

6.5.8 Characteristic features of high resolution NMR spectra in solids

In spite of the fact that the principles of the technique are the same, there are several factors causing significant differences between spectra of solids and liquids. In order to obtain high-resolution spectra in solids, specially designed spectrometers (or parts of the spectrometer) have to be used. Although it is possible to use the same spectrometer for both solution and solid state studies (and nowadays the manufacturers are developing systems which can easily be modulated for any technique like solution state NMR, solid state NMR, NMR Imaging, NMR Microscopy, or Localized NMR spectroscopy), usually each customer configures a particular spectrometer for only one experimental technique. The fact that in practice the spectrometers are dedicated either to solution or to solid state, contributes to the relative separation of these two fields in terms of dedicated teams. In general the solution state NMR is more often used than the solid state, and so are the number of available instruments. The same trend can be found in terms of books. We indicate some titles in solid-state NMR for the interested reader [23-25].

There are two factors we discussed previously and which affect in a very different way the spectra of solids. These are the relaxation time and the dipolar (through space) coupling.

The relaxation time associated with the signal decay is very short in solids. This is so because, on one hand the molecules are "packed" close one to another and are not separated by solvent molecules. In this way the magnetic nuclei are close to each other. On the other hand, the correlation time is very long, as there is almost no change in the position of various groups and atoms in solids. These two situations lead to a very fast relaxation process. As it was shown in Figure 12c, a short relaxation time gives rise to very broad lines in the NMR spectrum. In order to have a simple physical explanation for the broadening of the line, we can look to this phenomenon from the viewpoint of the lifetime in a particular state. Thus, once excited by the r.f. pulse, the nucleus is in another energy state. The relaxation time determines the lifetime of the excited nucleus. According to Heisenberg's uncertainty principle as the lifetime of a certain particle is shorter, the uncertainty of its energy is greater. In our case this means that a shorter lifetime induces a higher uncertainty in the energy gap ($\Delta E'$) between the two states of the nucleus and thus a greater uncertainty in the resonance frequency ($\Delta\nu'$) in the spectrum, this resulting in a broader line (Figure 18).

The other factor mentioned previously is the through space dipolar coupling between magnetic nuclei. As it was shown (Figure 14) this interaction depends on the relative position of the atoms with respect to the external (B_0)

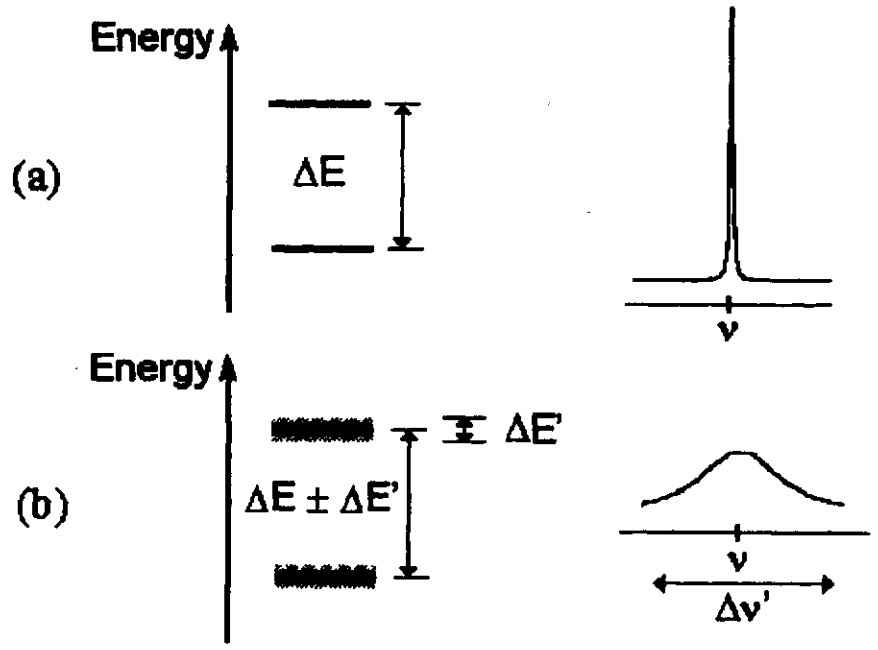

Figure 18: The influence of the lifetime of the nucleus on a particular energy level and the linewidth of the signal. a) if the lifetime and the associated relaxation time (T_2) is sufficiently long, the energy gap can be accurately measured and the position of the line in the spectrum can be well determined; b) if the time spent by the nucleus on a certain energy level is too short, the energy cannot be precisely measured and the line in the spectrum is broad.

magnetic field. In solids the molecules are not tumbling but rather occupy a fixed position in relation to the external field. This leads to the situation that the through-space coupling is no longer averaged to zero, so the spectrum will contain characteristic splitting patterns. However, the situation is still more complicated, as not all the molecules have the same orientation, but they are randomly oriented. As the coupling constant depends on the orientation of the molecules, a characteristic broad coupling pattern, named powder pattern, is present in solids (Figure 19). A coupling constant (K_{AB}), can be measured in this case. Moreover, if in the case of spin-spin (through bonds) couplings, chemically equivalent nuclei (*e.g.*, those in a CH_3 group) do not couple to each other, in the case of dipolar coupling, there are additional splittings generated by equivalent nuclei.

Another problem related to relaxation in solids is the following. Thus, one thing is the disappearance of the magnetization (M) in the x-y plane (the

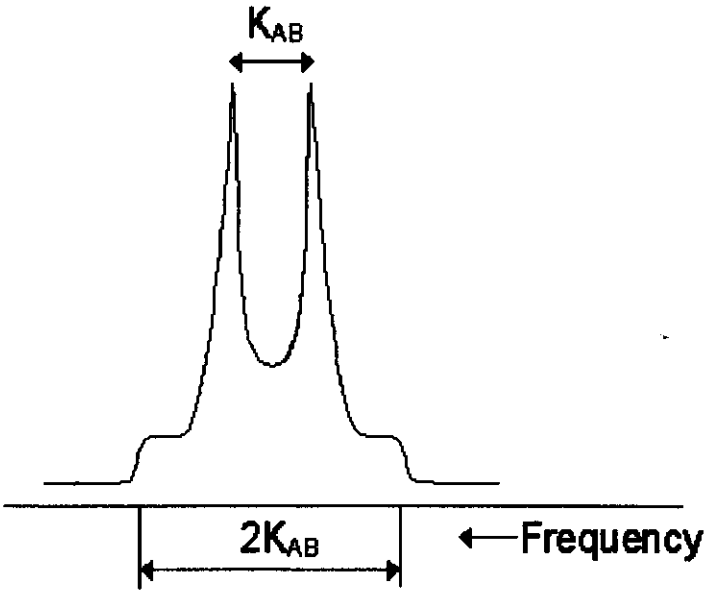

Figure 19: The characteristic powder pattern of the NMR signals in solids. The coupling pattern and the line broadening are due to the through space dipolar couplings.

signal detection plane), this being the short relaxation process discussed above, and a different process is the further relaxation of the magnetization along the z axis until its original magnitude (Figure 7 and section 6. 6). In solids this second process is very long in comparison with liquids. Although this process has no direct influence on the shape of the signal, it makes the experimental time very long because of the required relaxation delay.

There is still another factor contributing to the line broadening in solids which is worth being mentioned, namely the chemical shift anisotropy. Thus, the chemical shift of a particular nucleus depends on electron shielding. As the electron shielding also depends on orientation, and as all possible orientations are present in solids, this is an additional source of line broadening.

In order to overcome the problems arising from the factors described above and to obtain high resolution solid-state NMR spectra, special techniques and special spectrometer designs are employed. These differences will be mentioned in section 6.7.10 referring to spectrometer design.

6.5.9. Some common types of high resolution NMR spectra

We are presenting a series of one dimensional (1D) and two dimensional (2D) NMR spectra to exemplify the power of the technique. It is beyond the purpose of the present chapter to cover all types of NMR spectroscopy. Sometimes the same technique is known under several alternative acronyms, and in other cases different techniques provide the same information. We mention some of the most popular techniques listing alternative acronyms, but without detailing the full names or technical aspects. The interested reader should refer to already quoted books for more information [10,11,13]. A good compendium on basic 1D and 2D types of NMR spectra is Nakanishi's book [26] whereas some 2D-, 3D- and 4D-spectra are well explained in Evans' book [27]. However, as the techniques advance very fast, following more recent reviews and original publications is essential.

The Decoupling NMR experiment. Irradiation with a monochromatic r.f. having the same frequency as the resonance frequency of the nuclei in a particular group, produces the decoupling of the signals of the nuclei belonging to directly bonded groups. This technique simplifies the spectrum and facilitate the assignment of signals. Both homo- (same type of isotope being both irradiate and observed) and hetero-decoupling are usual.

The NOE spectra. The irradiation with monochromatic r.f. of the same frequency as the resonance frequency of one of the groups (but of lower power than that required for the decoupling experiment), produces an increasing intensity for the signals of the through-space neighboring groups.

2DNOE (NOESY). This type of spectrum produces the same information as a NOE spectrum, but showing all the connections in one spectrum. Another advantage is that one can see neighborhoods even for signals which are overcrowded or too close to be selectively irradiated. The spectrum appears as a square with spots located on the main diagonal which are projections of the signals of the normal ^{1}H-NMR spectrum (shown on the axes). These spots are named **diagonal peaks**. The off-diagonal spots, named **cross peaks** represent the NOE connections. Thus a NOE correlation is present if there is a cross peak connecting two diagonal peaks.

DEPT (APT) spectra. It is usual to record the ^{13}C-NMR spectra with broad-band hydrogen decoupling, thus removing the coupling patterns and showing only a singlet peak for each carbon atom in the molecule. The DEPT and APT spectra appear as "manipulated" ^{13}C NMR spectra, showing both positive and negative peaks, which enable one to assign various types of carbon atoms according to the number of hydrogen atoms being attached to them.

H,H-COSY spectra are looking similar to the **2DNOE** spectra, the diagonal peaks representing again the projections of all signals in the ^{1}H-NMR

spectrum (which is plotted on two edges of the COSY spectrum). The cross peaks in this case show only the correlations through bonds. Thus a COSY spectrum provides the information of a series of all possible homodecoupling experiments.

H,C-COSY (HETCOR, HMQC). This type of spectra provides a direct correlation between the signals of the carbon atoms and the signals of the hydrogen atoms directly attached to them (C-H). The normal ^{1}H-NMR spectrum is plotted along one of the edges and the ^{13}C-NMR spectrum is plotted along the other edge of the 2D spectrum. In this case the spectrum is no longer symmetrical and there are no diagonal peaks. The cross peaks provide the correlation information. The quaternary carbon atoms show no correlation peaks as they have no hydrogen atoms linked to them.

Long Range H,C-COSY (Long Range HETCOR, COLOC, HMBC). These spectra resemble the H,C-COSY one, the difference being that the cross peaks are no longer representing correlations between directly linked carbon and hydrogen atoms, but correlations over two or three bonds (C-C-H or C-C=C-H). Thus, some of the carbon atoms in the spectrum show correlation peaks with two different hydrogen atoms, as they have more than one different neighbor. Also the quaternary carbons show correlation peaks as they usually have neighbor hydrogen.

C,C-COSY (INADEQUATE, CCC2D). In this type of spectrum pairs of neighbor carbon atoms are linked by 2D peaks situated on the same parallel line. This is one of the most powerful 2D experiments enabling the entire carbon skeleton of a molecule to be mapped.

J-Resolved Spectroscopy. These spectra (either homo- or hetero-nuclear) are 2D spectra which allow the identification of coupling patterns and coupling constants. Each atom signal in the 1D spectrum plotted on one of the edges of the spectrum shows in the 2D spectrum a number of spots equaling the multiplicity of the 1D signal. Coupling patterns for otherwise overcrowded 1D spectra can be identified.

nD-NMR spectra.

We mentioned above only a very small part of the available 1D and 2D NMR techniques. Many other techniques are known not only as 1D and 2D but also employing more dimensions. We could for instance consider a 3D experiment H,H-COSY - H,C-COSY in which the peaks are spread inside a cube. Cutting the cube on a slice corresponding to the signal of one carbon atom would produce a COSY spectrum in which would be present only the H-H correlations of the hydrogen atom linked to the carbon atom for which the slice was selected. It is obvious that as we increase in dimensionality the

data are more and more spread thus interpretation of very crowded 1D spectra becoming easier.

6.5.10. Low resolution *versus* high resolution NMR

The parameters and phenomena discussed in the previous sections are common to all types of NMR spectroscopy (low- and high-resolution spectroscopy, solid- and liquid-state, localized or not, one- and multi-dimensional, imaging).

In principle, there is no clear cut border separating low resolution and high resolution spectroscopy. Resolution can be defined as the minimum distance between two lines in a spectrum at which they can be still distinguished. Starting from this definition and considering the dependence of the energy gap for the same nuclear transition on the magnetic field strength (Figure 5), we can see that the resolution increases continuously, as the external magnetic field increases. Thus, the number of distinct lines in a spectrum will increase for a particular compound and observed nucleus from one to the maximum possible number for that compound, as the spectrometer's magnetic field increases. In this respect one cannot define the minimum field for obtaining the maximum resolution otherwise than on a case by case basis. Moreover, as we mentioned in previous sections there are also other factors, like the homogeneity of the sample, viscosity of the solution and aggregation state which are dramatically affecting the resolution obtained for the same compound.

In common practice, in low resolution NMR our concern is with the analysis of the NMR signal in the time domain (FID) and the characterization of the physical structure of the bulk sample. The global relaxation behavior can provide extremely useful information on various aspects like the moisture determination or solid fat content. This global characterization of the sample in terms of molecular dynamics was the key to successful use of low field NMR in food sciences. Adding to this valuable information, the low cost of the low resolution instruments, the easy use of the instrument (not requiring special training), the specialized software (providing direct results to particular problems), one can hardly imagine a food chemistry department without making use of low resolution NMR spectrometers. It is thus easy to quote several analytical methods in food chemistry standardized on low resolution NMR spectroscopy.

The success of the high resolution NMR techniques was ensured originally by its extreme power in solving the structure of pure compounds. It is very often that the ultimate argument in determining the structure of an unknown compound is the NMR. Thus, the main applications of high resolution NMR are based on studying individual signals in the frequency domain (the common NMR spectrum). Relaxation measurements for individual signals

(thus combining the study of the time and frequency domains) provide valuable information both in terms of structural assignments and of mobility of various parts of the molecule. Interactions between different molecules (*e.g.*, identifying binding sites in biopolymers) are also common examples showing the power of the high resolution NMR. The main application of high resolution NMR in food sciences is in researches requiring structure assignment of newly isolated compounds. Adding to this restricted area the high costs of the instruments and also the high running costs, we can see the reason why the high resolution NMR instruments are not so widely used in food sciences as the low resolution ones. However in the early 1990s an increased interest was shown in studying complex mixtures (usually in solution) by high resolution NMR. This had a considerable impact in fields like food sciences and medicine.

6.6 MORE ON RELAXATION

As we have seen above, relaxation is a crucial process in the NMR technique. It is difficult to cover all aspects of the topic, but it is worth having a closer look to it.

Thus it is important to note that there are several mechanisms helping the excited nuclei to relax to the equilibrium state. The equilibrium state is the original distribution of atomic nuclei between the allowed energy levels (corresponding to allowed orientations) in the external and static magnetic field (B_0). There are at least two time constants characterizing the relaxation process. Thus the global time constant is called *the spin-lattice relaxation time* or *longitudinal relaxation time* (T_1) and represents the time required for the spin system to return exactly to the equilibrium state (Figure 6d-g and 4.4.e,h). The other relaxation constant refers to the return of the global magnetization (M) parallel to the z axis (*i.e.*, disappearance of the projection of magnetization in the x-y plane) as in Figure 7d,g. The time constant associated to this process is called *spin-spin relaxation time* or *transverse relaxation time* (T_2). As it is shown in Figure 20 the T_2 relaxation time can be either smaller then or equal to T_1.

6.6.1. Spin-lattice relaxation time (T_1)

The evolution of the projection of the magnetization (M) on the z axis (M_z) is described by the differential equation:

$$dM_z / dt = - (M_z - M_0) / T_1$$

After a pulse, the variation in time of the population difference (Δn) between the two states for a collection of spin 1/2 nuclei (Figure 5) can be considered an exponential growing according to the equation:

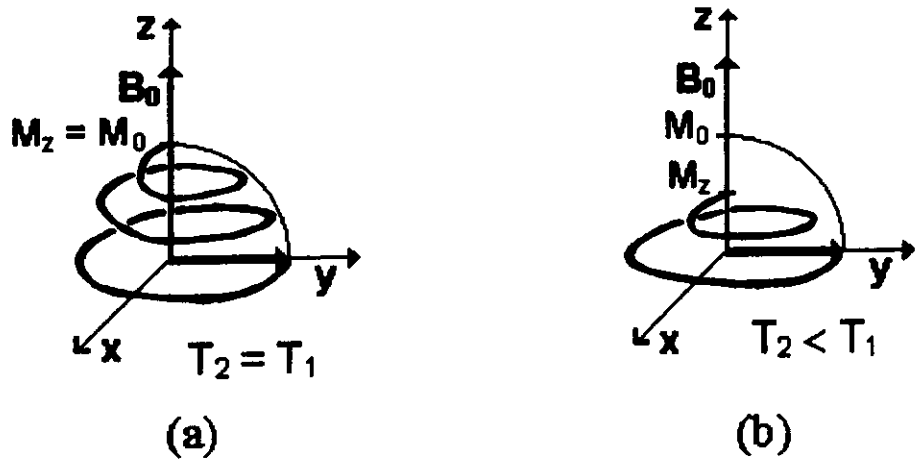

Figure 20: The relaxation process and magnetization trajectory for the case a) when spin-spin relaxation time T_2 equals the spin-lattice relaxation time T_1, and b) when spin-spin relaxation time is smaller than the spin-lattice relaxation time.

$$\Delta n(t) = \Delta n_{equilibrium}(1-e^{-t/T1})$$

The spin-lattice relaxation process is associated with the transfer of energy (which was previously absorbed from the external r.f. pulse), to the lattice (*i.e.*, the surrounding medium). The emission of energy is not spontaneous. Thus, the main mechanism leading to the dissipation of energy is the interaction of the excited spins with neighboring spins (dipolar coupling) in molecular motion. As the molecules undergo tumbling consisting of rotations, translations, vibrations and collisions with a wide range of velocities, and as the through-space dipolar coupling between magnetic nuclei depends on distance and position, the nuclei experience oscillating local magnetic fields (Figure 14). The oscillation of theses fields is modulated by the random tumbling motion. As there are a wide range of frequencies associated with these molecular motions, some of the motions have the right frequency to generate an oscillating magnetic field at the frequency of the NMR spectrometer (ν_0). It is this time dependent magnetic field that is responsible for the transition of the nuclei back to the fundamental state. Further, it is straightforward that the correlation time plays an important role in the probability to find the component of the molecular movement having the resonance frequency. Thus, a dependence of the relaxation time on the correlation time is expected to have a minimum for the optimum value of the correlation time (Figure 21).

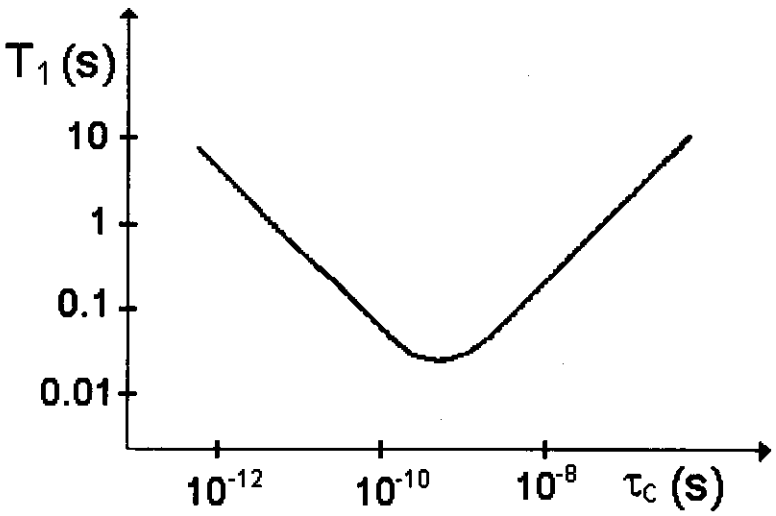

Figure 21: Dependence of the relaxation time (T_1) on the correlation time (τ_c). Left side of the plot is characteristic for small molecules in non-viscous solutions and the right side is characteristic for large molecules and viscous solutions.

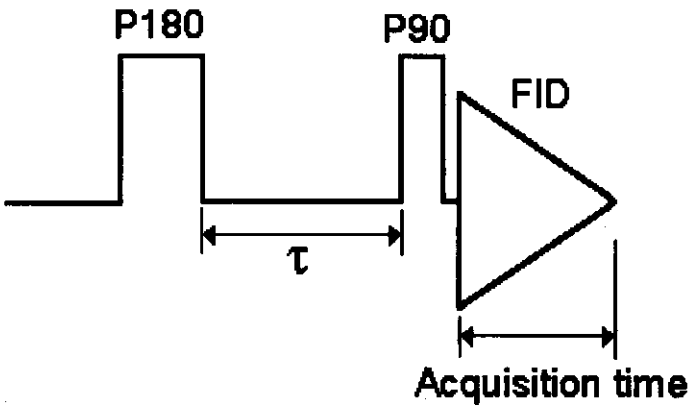

Figure 22: The inversion-recovery pulse sequence used for determination of the T_1 relaxation time.

The probability to find the right component of the frequency of the molecular motion for correlation times higher or smaller than the optimum value are

smaller, thus leading to longer relaxation times. For most small organic molecules in non-viscous solutions the situation is represented by the left side of the curve in Figure 21. Thus the molecular tumbling is fast (correlation time small) and conditions which slow down the motion are shortening the relaxation time. For large molecules (*e.g.*, long proteins) the molecular tumbling is rather slow and the normal situation is found on the right side of the plot in Figure 21. Thus, for such compounds, slowing further the motion is increasing the relaxation time. A reasonable short T_1 is desirable because it cuts down the experimental time and increases the sensitivity, but below a certain value, a too short T_1 broadens the lines, thus destroying the resolution. Estimation of T_1 values is essential for quantitation purposes. Thus one should employ a relaxation delay of at least 5 times the longest T_1 in the molecule in order to obtain accurate integrals for signals.

There are several methods for experimentally determining the T_1 relaxation time. We will briefly mention here the **inversion-recovery** technique (Figure 22). In this technique two pulses have to be employed. A first pulse (P180) having the appropriate length turns the magnetization by 180° (Figure 6c) and after a variable delay τ, another pulse (P90) having the appropriate length turns again the magnetization by 90°. After the first pulse (P180), during the τ delay, the magnetization freely evolves toward the equilibrium position (Figure 6d-f). The projection on the z axis of the magnetization during this relaxation process decreases along the -z axis, reaches the zero position and then increases along the +z axis until it reaches the initial value M_0 (Figure 6g). A series of experiments is repeated with stepwise increasing values of the τ delay. After each τ interval a P90 pulse is employed and the signal generated by the magnetization immediately collected by a detector situated on the y axis. For the situations when after the τ delay the magnetization on the z axis did not reach the zero value (Figure 6d), a new pulse (P90) in the same direction as the previous one (along x axis) further turns the magnetization (clockwise) toward the negative y axis. Thus the detected signal produces a negative line in the spectrum. The negative signal stepwise decreases in intensity as the τ delay increases and the magnetization (M_z) before the second pulse approaches the zero value. For a certain value for τ, when the magnetization has exactly zero value (Figure 6e), no signal is detected on the y axis. Further increasing the τ interval leads to a progressively increasing positive signal detected on y axis, as the P90 pulse turns the magnetization on the positive y axis (Figure 6f). After a certain value for τ, when the magnetization reached the M_0 initial value, further increasing this delay produces the same positive intensity for the line in the spectrum (Figure 6g). The plot of the intensity of the signal as a function of τ matches a curve similar to that shown in Figure 7e, with the exception that the experimental curve shows an arbitrary scale for the z axis, representing the intensity of the signal in the spectrum, and not the actual value for the magnetization. It can be shown that the relationship between

the value of the τ delay for the point when the intensity of the detected signal is zero (τ_0) and the T_1 relaxation time is:

$\tau_0 = T_1 \ln 2$

6.6.2. Spin-spin relaxation time (T_2)

This relaxation process refers only to the period required for the projection of the magnetization (M) into the x-y plane (M_{xy}) to vanish. In other words T_2 is the time required for the magnetization M to realign along the z axis (Figure 7c,d). As the signal detector is placed along the y axis, it is thus the T_2 which determines for how long the NMR signal (FID) lasts (Figure 7d,g). As we have seen previously, the relaxation time T_2 has a major influence on the linewidth. In other words, we cannot measure very precisely the frequency of a signal which lasts for a too short period, thus a short T_2 give rise to broad peaks:

$\Delta\nu_{1/2} = 1 / \pi T_2$

If the effect of T_2 on the NMR spectrum is not so difficult to understand, the mechanism for the vanishing of the M_{xy} projection of the global magnetization M is rather complex, and there are several factors affecting this process. It is essential to note that T_2 cannot be longer than T_1 (Figure 20).

As T_2 is usually shorter than T_1 there must be some additional factors contributing to the relaxation process associated with T_2. The mechanism by which T_2 is decreasing in the x-y plane, without affecting the z projection, is a fanning (or dephasing) of the global magnetization vector. Once the vector M was tipped under a certain angle α by an r.f. pulse (Figure 23a), the projections of the M vector are M_z and M_y, the component on the x axis (M_x) being zero. The projection in the xy plane (M_{xy}), in this case equals the M_y projection. Once the r.f. pulse turned off, the magnetization begins to relax. In this moment one of the natural tendencies for the global magnetization (M) is to rotate (precess) around the z axis (which is the direction of the external magnetic field B_0). If we ignore the other tendency (namely to align the vector M along the z axis), the result is a precession around the z axis under the same tip angle α (Figure 23b). In this situation the M vector remains constant, and also constant remain the two projections M_z and M_{xy}. The other projections M_x and M_y are not constant, but they oscillate between a maximum positive and a minimum negative value equal to M_{xy}. Figure 23c shows the same situation as in Figure 23b, but viewed as a projection in the xy plane. In order to explain a decreasing of the M_{xy} component of the magnetization M while leaving the M_z component constant, we have to consider a spreading of the M vector into several components pointing in different directions on the same circle (Figure 23d). In this case the

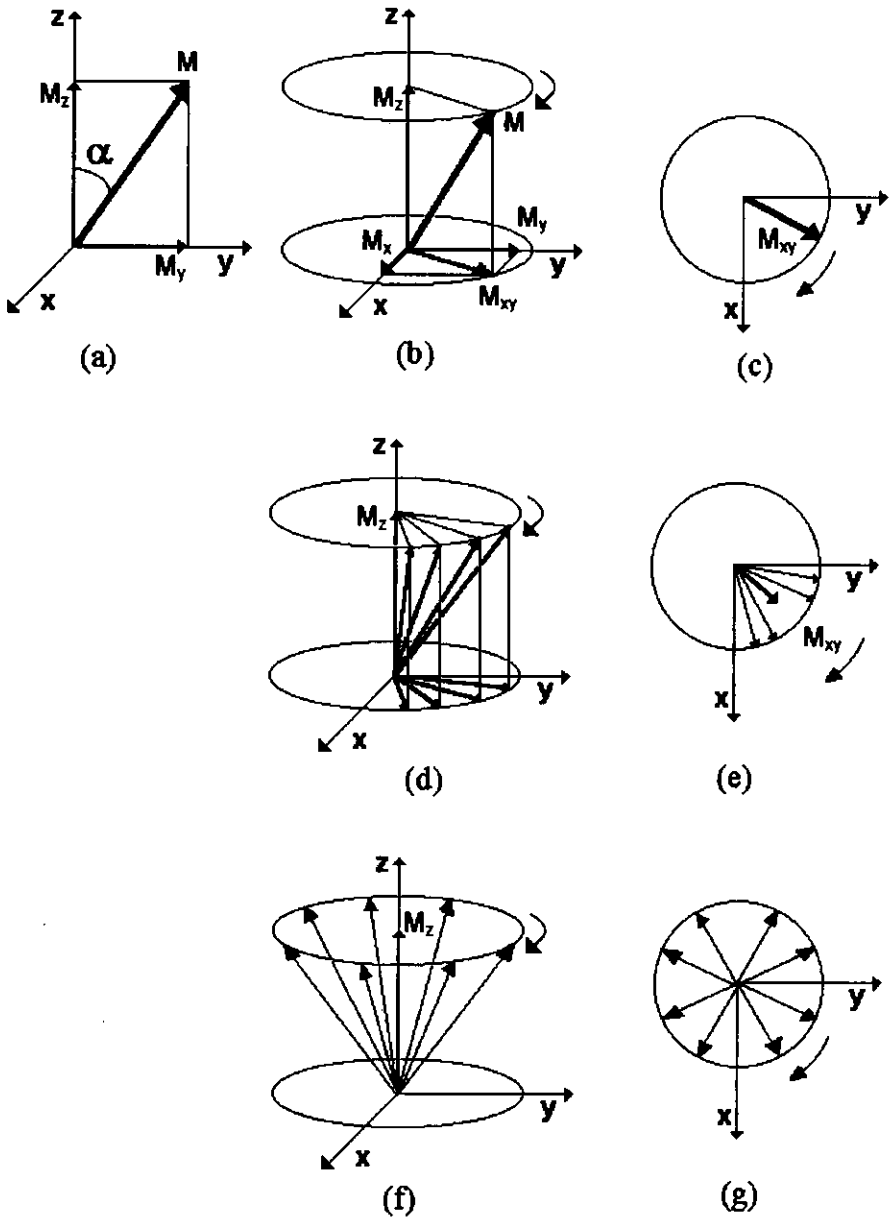

Figure 23: The relaxation process associated with the T_2 time constant. The external magnetic field B_o, which is not explicitly shown, has the same direction as the z axis. a) an r.f. pulse flips the magnetization vector *M* by an angle α away from the equilibrium position; b) once the pulse turned off the magnetization freely precess around the z axis. c) the same situation as in the previous figure but viewed as a projection in the x-y plane; d) not

Figure 23 cont:

all the molecules in the sample experience the same external magnetic field, thus there are several components of the magnetization precessing with different speeds. This situation leads to a fanning of the magnetization vector which is increasing in time. e) the same situation as in the previous figure, but viewed as a projection in the x-y plane; f) after a sufficiently long time the fanning process reached the situation when the magnetization vector is uniformly spread on the rotation cone around the z axis. The projection on the z axis was not affected, but the projection in the x-y plane vanished; g) the same situation as in the previous figure viewed as a projection in the x-y plane. Individual components of the magnetization are canceling in this plane.

projection on the z axis M_z is unaltered, as the individual components have a common projection on the z axis. If we consider however the components in the x-y plane (Figure 23e), it is clear that the sum of the individual projections which is the global M_{xy} component, is smaller in this case by comparison with the previous situation. If the process of fanning out continues, eventually it is reached the situation when the M vector is equally spread on the surface of the rotation cone around the z axis (Figure 23f). Again, this situation does not affect the M_z component, but the sum (M_{xy}) of the individual projections in the xy plane is zero (Figure 23g). In fact we reached the situation when the magnetization is fully relaxed in the xy plane. There are several factors affecting the dephasing process, and (contrary to the T_1 relaxation mechanism), dephasing not necessary requires dissipation of energy, thus the T_2 process can be faster than T_1.

One of the factors affecting the dephasing and thus, contributing to the T_2 relaxation time is the spin-spin interaction. Chemical exchange phenomena (when present) contribute very significant to the shortening of T_2. Scalar coupling (J-coupling) is another source for T_2 shortening.

This relaxation time is very important as it is associated to the "natural linewidth". However the time constant T_2 cannot be directly quantified, because there are other factors which also contribute to the dephasing process. These factors are experimental factors and are related to the inhomogeneity of the B_0 field in the sample. As different molecules in the sample experience slightly different B_0 fields, their precession frequency (and resonance frequency, ν_0) is slightly different, thus the dephasing is faster, T_2 becomes shorter, and the actual line in the spectrum is artificially broadened.

As a result of the superposition of internal (sample's characteristics) and external (experimental) factors affecting the T_2 process, by measuring the half-height linewidth we can deduce only a global T_2 time denoted as T_2^*:

$$\Delta\nu_{1/2} = 1 / \pi T_2^*$$

The same is true if we consider the time required for the FID signal to vanish (Figure 7d,g) when we would again obtain the T_2^* rather than the T_2 time constant.

In order to obtain the natural T_2 constant (which is a function only of the molecular characteristics of the studied compound) we should subtract the artificial contribution of the experimental factors (field inhomogeneity) from T_2^*.

An experimental method for measuring the T_2 constant is the **spin-echo method**. Briefly, the idea is to do "something" (at some stage in the development of the experiment), to invert for a while the effect of the inhomogeneity of the external field. The result would be that the dephasing effect, inverted but with the same magnitude, would produce a refocusing of the magnetization. Figure 24 presents the evolution of the magnetization during a spin-echo experiment. The pulse sequence includes a train of one 90° pulse (P90) and two 180° pulses (P180) separated by appropriate delays (τ) and the acquisition time (Figure 24a). The experiment begins with a 90° pulse (P90) which turns the magnetization along the y axis (Figure 24b,c). At this moment the magnetization in the x-y plane (M_{xy}) equals the initial magnetization vector (M_0) as magnitude. The magnetization begins to dephase, some components rotating faster, others slower (Figure 24d). After the time τ the first 180° pulse (P180) is employed. In this way the fanned magnetization is turned around the x axis (Figure 24e). The fanned magnetization continue to evolve with different speeds as a result of the experimental inhomogeneities. However, as they have been rotated with 180°, the last components of the magnetization have the fastest movement, and the first ones the slowest movement. Thus after exactly the same time interval τ, the magnetization refocuses (Figure 24f). The only difference is that the M_{xy} magnetization is shorter than the original M_0 vector. This shortening is due to the "true" T_2 relaxation process generated by the intramolecular factors. At this point the magnetization M_{xy} continues to evolve and the field inhomogeneities which refocused the vectors, are now further defocusing them, as the individual components continue to rotate (Figure 24g). After another τ time interval, a second 180° pulse is applied (Figure 24h), the M_{xy} magnetization refocuses again (Figure 24i), this time even shorter in magnitude, and the process continues (Figure 24j) while the signal is detected. In fact large numbers of 180° pulses are employed. The experiment is repeated, beginning with only one 180° pulse and each new

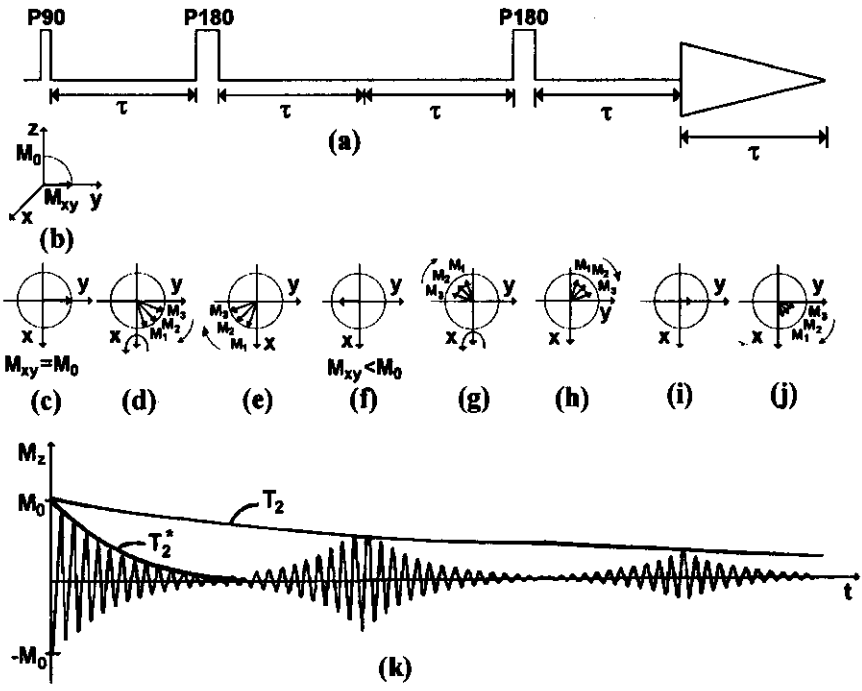

Figure 24: a) The spin-echo pulse sequence; b) and c) the first 90° pulse turns the initial magnetization M_o along the y axis; d) during the first τ interval the magnetization defocuses e) the first 180° pulse turns the magnetization around the x axis, thus inverting the ordering of the individual components; f) after another τ interval the magnetization refocuses; g) the further free evolution defocuses again the magnetization; h) after the second 180° pulse the magnetization is again inverted; i) the magnetization refocuses one more time; j) the defocusing takes place while the FID is recorded; k) the evolution of the magnetization in time during the spin-echo experiment and the two time constants T_2 and T_2* associated with this process.

experiment contains a new 180° pulse. In this way, each FID collects a further and further echo. Plotting the amplitude of the signal generated by each echo as a function of time allows the determination of the T_2 relaxation time, not affected by experimental imperfect conditions (Figure 24k). The much faster relaxation time for individual echoes is the T_2* relaxation time (Figure 24k).

6.7. INSTRUMENTAL AND EXPERIMENTAL CONSIDERATIONS

A schematic diagram of a NMR spectrometer is presented in Figure 25. Depending on the type of spectrometer some elements may be missing or additional ones may be present.

6.7.1. The spectrometer

One way to characterize the spectrometers is in relation with their type of magnet. Thus, there are permanent, resistive (electromagnets) and superconducting magnets. Another way is to specify the way of excitation of the sample. In this respect there are Continuous Wave (CW) and Pulse systems (PFT). Two different constructive types of CW spectrometers are also possible: with Magnetic Field Sweep (at fixed frequency) and with Frequency Sweep (at fixed magnetic field). Another way to characterize the NMR spectrometers is based on the mathematical treatment of data. Thus, there are spectrometers either with or without mathematical treatments. Nowadays Fourier Transform (FT) is a standard feature of spectrometers and some advanced systems have additional non-FT processing methods (Linear Prediction, Maximum Entropy Method, Hilbert Method, Bayesian Analysis). Still another way to characterize an NMR spectrometer is according to the field strength. Thus, there are Low Resolution and High Resolution spectrometers. The High Resolution are usually referred as low-, medium-, high- and ultra high-field spectrometers. NMR imaging and microscopy are already considered separated topics, and usually (because of the vastness of the field) treated separately in most discussions. There is still another NMR technique, namely localized NMR spectroscopy, which is sometimes treated as a branch of NMR spectroscopy, other times as a branch of NMR imaging. As we are not covering imaging in this chapter, we can again distinguish between two types of NMR spectroscopy (and spectrometers), namely localized- and non-localized- NMR spectroscopy.

6.7.2. The magnet

All types of magnets (permanent, resistive and superconducting) are presently used. For low resolution both permanent and resistive magnets are used. For high resolution low field (usually, up to 80 MHz, although theoretically up to 100 MHz), the tendency is to use electromagnets. Some permanent magnets are still in use in rather isolated cases. For fields higher than 100 MHz, only superconducting magnets can be used.

Permanent magnets generate a very stable magnetic field, but they should be well thermally insulated, and they are very heavy. They have been the most commonly used instruments until mid 1970s. Electromagnets, are lighter,

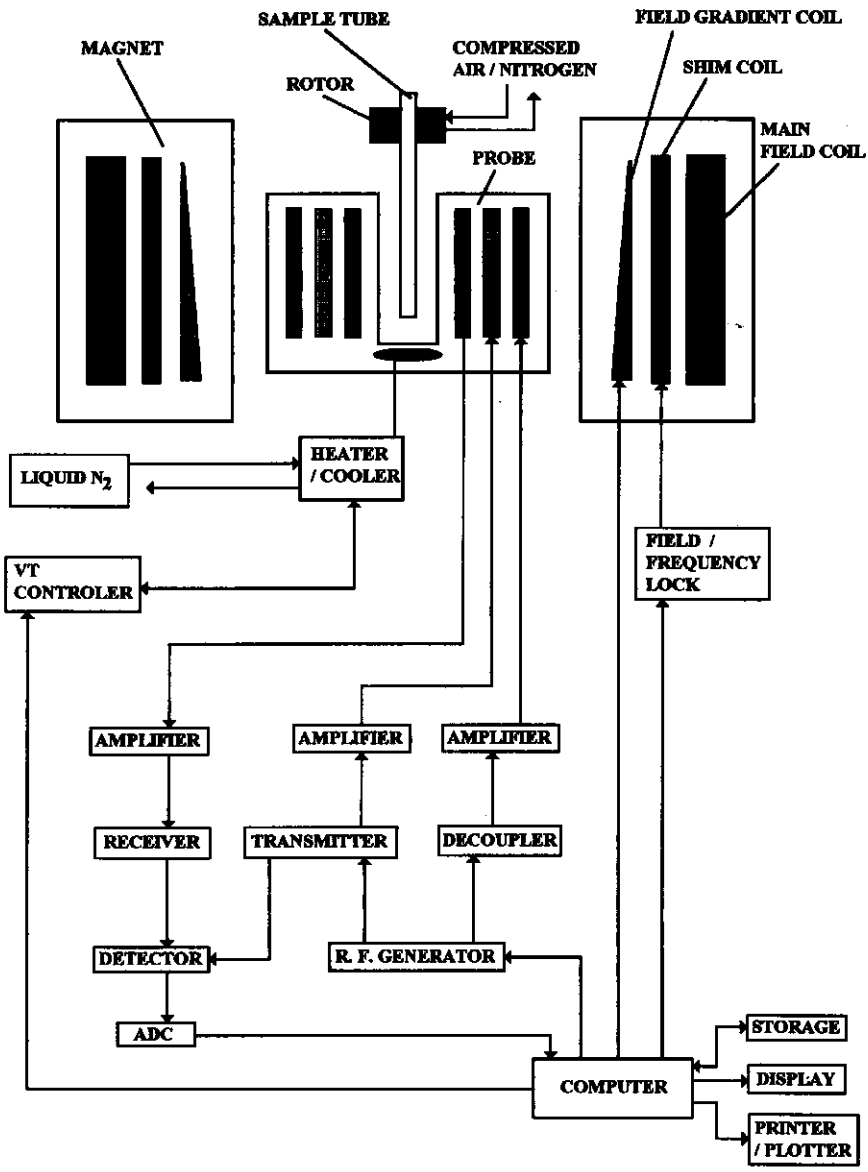

Figure 25: Block diagram of a high resolution NMR spectrometer.

but require an additional power source and a water-based cooling system. In order to ensure the required stability of the field an additional system of locking the field on the NMR signal of a nucleus in the sample which is not recorded is used in most of the cases. Commonly the field is locked on the deuterium signal of the solvent. Superconducting magnets are the only

available choice for fields higher than 100 MHz, because iron saturates at 2.35 T. Commercially available field strengths goes up to 800 MHz. Major advantages lie in the wide spread of signals, extremely high field stability (using the same locking system as the electromagnets), high resolution and sensitivity. The magnets are very light. Once energized, the superconducting magnets do not require an additional power source anymore. A major constraint introduced with the use of superconducting magnets comes from the need to cool the niobium-titanium coil with liquid helium. They also require liquid nitrogen for slowing down the evaporation rate of the liquid helium. Therefore an important characteristic of a superconducting magnet is the time interval between helium refills. The usual refill interval for liquid nitrogen is two weeks, whereas for liquid helium varies between two months and one year, depending on the type of magnet. However one can regard the superconducting magnets as more nature-friendly than the electromagnets because they do not waste water.

Apart from the coils generating the main magnetic field, the magnet has additional coils named shim coils, which generate additional weaker magnetic fields intended to compensate the inhomogeneity of the main magnetic field and the inhomogeneities introduced by the other components (probe, sample tube, sample, *etc.*).

Depending on the type of spectrometer and experiments desired, additional coils named field gradient coils can be also used. These coils are very common in (and have been first designed for) NMR imaging, but are essential for localized spectroscopy as well. Using such coils the homogeneity of the main magnetic field can be deliberately destroyed (making the field to continuously increase from one side of the sample to the other by a certain gradient) so that the resonance condition can be selected for only localized regions of the sample. Thus NMR spectra can be recorded for regions of the sample rather than for the average sample how is usually the case. This is of tremendous importance for nonhomogeneous samples as some food samples are.

6.7.3. The probe

The probe's various coils both transmit and detect the r.f. signals, and regulate the temperature. The number of coils depend on the purposes for which the probe is designed. It is also common that one coil has more than one function, *e.g.* both transmission of the pulses and detection of the signal for a particular nucleus. A wide range of options is available in terms of NMR probes, according to the type of experiment required (*e.g.*, type of nucleus, number of channels and thus the maximum number of dimensions in a spectrum that can be recorded, amount of sample, type of detection, temperature and pressure ranges, coupling with other analytical instruments, solid or solution state, *etc.*).

Once the spectrometer purchased, the probe is the most important part which could improve the spectrometer's performance. Upgrading the probe with latest generations can dramatically increase spectrometer's performance and this is the main way of coping with the progress of the technique.

6.7.4. The computer

As in any high technology, computers are one of the most important leading forces in the advancement of scientific equipment. Advancement in computers made possible the development of commercial pulse FT-NMR spectrometers in early 1970s, although the pulse methods have been known since late 1940s. In 1987 processing one of the first 3D-NMR spectra took seven hours and in 1990 a 4D-NMR spectrum was reported to require sixty two hours of computing. Nowadays these experiments can be performed routinely with latest generations of commercial NMR spectrometers, mainly because of advancement in computers and software. Until late 1980s the NMR computers were dedicated system computers. Since early 1990s all modern high resolution spectrometers are using standard workstations, and networking several such workstations and the NMR magnet is a common practice. Latest generations of low-resolution NMR spectrometers have usually a dedicated computer, but they have an interface allowing direct linking with common Personal Computers. Upgrading the computer is probably the second action after upgrading the probe, which must concern somebody wanting to extend the lifetime of an instrument. The third important action in the same direction is upgrading some electronic parts. Last action on the list is replacing the magnet.

6.7.5. The analog-to-digital converter

The NMR signal (FID) is detected by the Receiver as an electrical signal. This signal is transformed by the analog-to-digital converter (ADC) into numbers which can be further stored and manipulated by the computer. The ADC determines both the maximum spectral width which can be recorded by the spectrometer (a typical value is 150 KHz), and the dynamic range of the spectrum. The dynamic range is the difference in intensity between the highest and the smallest signals in the spectrum for which the smallest signal can still be recorded. Signals which are smaller than this minimum intensity are not collected as signals by the spectrometer regardless how many scans are accumulated.

6.7.6. The software

The software is continuously developed by the spectrometer manufacturers as part of their NMR system development. This software allows better and better control of the hardware and design of NMR experiments. Also, the same software development allows better and easier treatment of data (FID)

once the NMR experiment finished. For this second part of post processing, there are also third software companies developing their independent NMR processing programs. Common features of such post processing software include baseline correction, peak fitting, lineshape analysis, slice selections and peak projections, resolution or sensitivity enhancement, library searches and spectral matching, conversion of data between various types of instruments, simulation of NMR spectra and comparison with experimental ones, calculation of chemical composition of the sample or some physical properties, *etc.*

6.7.7. The Sample

For high resolution spectra sample handling is very important. As the homogeneity of the sample is critical, ensuring very well mixing with the solvent is very important. Filtration of the sample has to be employed quite often. For very dilute samples, contamination problems should be considered (*e.g.*, acetone from the washing process, or sweat from the fingertips). Degassing the sample is critical in some experiments. Avoiding the presence or on the contrary, deliberately adding paramagnetic species to the sample are also options which have to be taken in relation to the type of experiment performed.

Sample volume is also important. Each probe has a specific detection coil that receives signals from only a finite volume in the core of the magnet. There is an optimum volume, greater than this detection coil volume which minimizes field distortions caused by the solution/air interface. When enough sample is available, this optimum volume should be used. For samples in small quantities, other strategies can be used (*e.g.*, capillary tubes, vortex suppressers, microprobes, *etc.*).

When enough sample is available, the concentration is chosen depending on the information desired. Thus, high concentrations are desired for good signal-to-noise ratios (*e.g.*, nuclei with low natural abundance), for short recording times and for some two dimensional experiments (*e.g.*, H,C-COSY, COLOC, INADEQUATE). On the other hand, dilute solutions are preferred for higher resolution spectra, NOE experiments and other two dimensional experiments (*e.g.*, H,H-COSY).

6.7.8. The solvent

The routine high resolution NMR spectrometers lock the magnetic field on the deuterium frequency of the solvent. Although other techniques exist, the use of deuterated solvents is the best choice (when possible), as it gives better quality spectra.

Apart from the solubility of the sample, other factors should be considered when choosing a solvent. The price plays an important role as it varies greatly from one solvent to another. The viscosity of the solvent has an important effect on the resolution of the spectrum. Viscous solvents usually produce lower resolution spectra than non-viscous ones. The usual non-viscous solvents are: acetone-d_6, acetonitrile-d_3, chloroform-d, dichloromethane-d_2, and methanol-d_4. Usual viscous solvents are: benzene-d_6, dimethylsulfoxide-d_6, dimethylformamide-d_6, pyridine-d_5, toluene-d_8, water-d_2. In some experiments the number of deuterated atoms per molecule of solvent has to be considered. For instance a higher strength of the deuterium signal (*e.g.*, acetone-d_6 *versus* chloroform-d) is better for NOE experiments and for cases when the deuterated solvent is added in a small quantity to another undeuterated solvent. The boiling and melting points have to be considered when variable temperature experiments are planned. The position of the residual undeuterated solvent signal as well as the deuterium content have to be considered for samples in very small quantities. The presence or absence of water traces in the solvent may be relevant in some cases (*e.g.*, use of shift reagents, sensitive samples).

6.7.9 The sample tubes

The quality of the tube (*e.g.*, concentricity, wall thickness) is very important when very good resolution is required. Also, each type of probe has a lowest recommended quality sample tube and the use of lower quality tubes can lead to the damage of the probe. Each manufacturer specifies the quality parameters in terms of inner and outer diameters, wall thickness and concentricity. Each product has a specified tolerance for these parameters. Apart form the catalogue quality, the history of the tube is also very important (*e.g.*, how it was cleaned, dried, stored, even what samples have been previously analyzed in it, as these operations might lower its quality).

6.7.10 Special characteristics of high resolution solid-state spectrometers

As it was shown previously (section 6.5.8), some characteristics of the solid state make the NMR spectra look different for solids than for liquids. In order to obtain high-resolution spectra the following technical features are used.

Dipolar interactions (leading to coupling patterns between nuclei which are not directly bonded) can be minimized by using high-power decoupling fields. If the decoupling power usually employed for liquids is about 5 W, typically 50 -100 W are required for solids.

Broadening due to chemical shift anisotropy can be reduced using the magic-angle-spinning (MAS) technique. MAS involves very fast spinning of the

sample under an angle of 54.7° to the applied magnetic field. Normal spinning rate for liquid samples is 10 - 20 Hz, whereas for solids it is in the range 10 - 20 kHz, which means a supersonic speed.

Relaxation times can be reduced by a technique named cross-polarization (CP), which results in polarization transfer between highly polarizable ^{1}H-nuclei and the observed nuclei (usually ^{13}C).

Nowadays, ^{13}C-CPMAS NMR spectra are routinely recorded and most of spin 1/2 nuclei are accessible. Although not yet a routine practice ^{1}H and ^{19}F as well as two-dimensional spectra can be also recorded.

For solid state NMR, small ceramic rotors are used instead of classical sample tubes.

6.8 FUTURE TRENDS

It is difficult to make predictions on how the NMR field will develop. The variety of techniques, applications and instrumentation available today was hard to imagine only a few years ago. We will briefly mention some tendencies which could also be relevant for food sciences. But certainly the future will show much more than that.

The current state of the instrumentation could be summarized as follows. Samples can be investigated in all states: gaseous, liquid, dispersions in liquid, gels, solids. NMR spectra of practically all isotopes magnetically active have been recorded. The highest magnetic field commercially available is 800 MHz. The temperature that can be reached in specially designed NMR probes exceeds 2,000°C using laser-heating systems. High pressure NMR experiments can be carried at 10,000 atmospheres. The dynamic range has been pushed well above 10,000 : 1. The NOE enhancements of less than 1% are easily detectable. 3D experiments are routine and 4D experiments are often performed.

There is every reason to believe that both instrumental and theoretical aspects of NMR will continue to progress. New pulse sequences will be invented, computer power will continue to grow and field strength and homogeneity will increase. Already there is a project for building a 1,000 MHz spectrometer. Special design of the building, parking and even roads around that site are carefully considered in order to prevent the interference with the magnetic field. Probably, this will remain a unique project for a while, but it is likely that 800 MHz instruments will become popular in the next few years.

Although many efforts are directed toward increasing the magnetic field strength, it is worth mentioning an interesting aspect. Apparently increasing

the magnetic field does not necessarily increase the resolution. This statement might look somehow strange. There are some reports that running NMR spectra on large molecules (proteins) at 750 MHz, do produced a slightly worse resolution than at 600 MHz. The explanation seems to be the fact that chemical shift anisotropy may become the dominant mechanism for spin-lattice relaxation above a certain level of the magnetic field, thus the increase in line broadening becoming faster than the increase in chemical shift separation. This phenomenon might set (at least theoretically) an upper limit for some ^{1}H NMR studies (and other nuclei like ^{31}P). This would be true for large molecules and if a field strength limit would be reached this is likely to be set for biochemical studies rather than food fluids. For complex mixtures of small and medium size compounds, this anisotropy does not arise and we have every reason to state that NMR spectra of such mixtures should be run at the highest available magnetic field.

Further improvements in software are also to be expected. This will lead to both better hardware control and the post processing of data. There are already examples of controlling the spectrometer from a remote PC, but this is not yet a standard feature. Probably, in the future the workstations will cease to have the monopoly over instrument control and this will be possible without any compromise using PCs, with all the benefits these computers have in term of costs, popularity and software compatibility.

It is a general consensus that a new revolution in instrumentation is to be expected once the new materials with superconducting properties at the temperature of liquid nitrogen will be introduced.

A new application will probably become very popular quite soon. This is the magic-angle-spinning (MAS) spectra of non-solids. The benefit would be for all heterogeneous samples, polymers in suspension, gels, viscous liquids, *etc.*. Special probes for MAS of quasi-liquids have been already designed. Probably this is the signal for a new development stage in the NMR field which will make the combined solution- and solid-NMR spectrometers to become popular and often used by "solution state spectroscopists".

Localized spectroscopy will also steadily grow in popularity and be used in connection with solid or quasi-liquid techniques.

Coupling Liquid Chromatography with NMR is another field which is steadily growing. HPLC-NMR probes and accessories are already commercially available and it is a strong competition to develop this exciting new technique. Less then 150 ng can now be detected with such systems.

Non-FT FID processing will be more frequently used as the commercial spectrometers tend to include them as options in the standard configuration.

3D and 4D experiments will become very popular and the increase in dimensionality will continue.

Pulse Field Gradient techniques, as well as digital lock and digital filtering already became standard options for last generations of instruments.

Spectral width, dynamic range, resolution and sensitivity are expected to be pushed toward further and further limits.

Probably soon we will have to reconsider standard sentences as "the relatively low sensitivity of the method" or "the limited use of less sensitive nuclei". The nuclei to be recorded will be more and more often chosen on the exclusive basis of the information provided, and not on their "accessibility" as it is usually the case now.

Automation will continue to develop and the "black box" which is now the modern NMR spectrometer for most of the users might become even blacker as the computers and software become more and more user-friendly. More standardized analytical methods will be based on both low and high resolution NMR methods. Better shielded magnets will probably be developed and NMR will eventually be introduced in factories and more widely used for on-line quality controls.

Many of the "research" and high-resolution techniques will percolate to "routine" and low resolution. There are studies demonstrating that NMR can be successfully used to characterize complex mixtures, and when used with automatic sample changers and specialized software packages, the cost of the method can compete with other techniques. Adding to this cost-related aspect, some information which can hardly be obtained by other techniques (like the geographical origin of wines or the fatty acid distribution among the three possible sites of a triglyceride) and we should expect an increasing use of high resolution NMR techniques in food sciences in the years to come.

Another relatively new application is the so called Site Specific Nuclear Isotope Fractionation (SNIF) studied by NMR. This approach gained a wide recognition when it was proven to provide valuable information on the geographic origin of wines and on the synthetic *versus* natural origin of some food ingredients. The principle of the method is to measure the isotope ratio for a particular element (*e.g.*, ^{1}H to ^{2}H ratio). It is likely that SNIF-NMR techniques will be more and more extensively used for both product authentication and identification of origin. The extension of SNIF-NMR to ^{13}C as a more routinely technique will greatly improve the discrimination power of the technique.

Hybrids of NMR and other techniques (*e.g.*, atomic force microscopy) will probably lead to development of new and independent research fields.

6.9 APPLICATIONS OF NMR TO FOOD ANALYSIS

Relative to most other techniques discussed in this book, NMR has found a limited number of "niche" applications in food analysis. For example, the determination of oils is seeds (or fat in chocolate!), based upon low resolution, solid phase NMR is well used in quality control laboratories. Actually, most applications that found their way in food analysis are methods based upon the differences in relaxation times of various molecules (*e.g.* free water molecules *versus* bound water molecules). Consequently, for the purpose of this particular chapter, we shall discuss only two specific applications of NMR to food analysis. These examples were chosen solely to demonstrate the broad range of applications that NMR can cover and the reader is advised that the mere fact that they were selected here should not be interpreted as a judgement of their value over other related references.

6.9.1 Characterisation of ginsenosides by high resolution ^{1}H NMR

Panax spp., especially *Panax ginseng*, are purported to possess various health benefit qualities. In oriental countries it has been used as a traditional panacea for numerous health disorders for several centuries. Saponins are generally recognised as the main effective components of ginseng. Because of their close similarities in terms of structure they offer a real challenge to the analytical chemist in terms of separation. Furthermore, the relative complexity of their structures makes them perfect candidates for in-depth structural characterisation work by NMR.

A few years ago, while affiliated to a food research facilities, we carried out extensive work on the suitability of food irradiation for various foodstuffs. As part of an agreement with the International Atomic Energy Agency (IAEA) in Vienna, aiming at training foreign food scientists in the area of food irradiation, we undertook extensive studies related to the treatment of ginseng (*Panax ginseng*) by ^{60}Co (γ-rays) for the purpose of extending its shelf-life [28, 29]. During the course of these investigations we extracted and isolated several types of components including various known, and unknown ginsenosides.

The aglycones moiety of ginsenosides are of the dammarane triterpenes family (Figure 26). The actual ginsenosides are divided with respect to the level of substitution of the aglycone. We reported earlier NMR-based structural elucidation work [30] where we presented original proton-NMR data on various ginsenosides. Full assignment of the structure was possible only after combining a variety of spectra such as standard 1D ^{1}H and ^{13}C spectra, DEPT (using either a 135° or a 90° reading pulse [31]), COSY (or long-range COSY) [32], double-quantum filtered COSY [33, 34] with or without phase-sensitive detection using TPPI [35, 36], COSY with one, two, and three relay coherence transfer steps [37, 38], double-quantum spectroscopy [39], NOE difference

spectroscopy, 2D ROESY [40, 41], 2D heteronuclear ^{13}C-^{1}H correlation (HETCORR) [42], and carbon-hydrogen correlations from one-dimensional polarisation transfer spectra by least-square analysis (CHORTLE) [43]. To appreciate the complexity of the problem at hand, one must look at the structure of such compounds, or more simply, to look at their IUPAC name. For example, the nomenclature for the so-called ginsenoside Rb_1 is as follows: (3)-[β-D-glucopyranosyl(1→2)-β-D-gluco-pyranosyl]-(20)-[β-D-glucopyranosyl(1→6)-β-D-glucopyranosyl]-20S-protopanax-diol.

Figure 27 provides an example of one two-dimensional NMR spectrum. It depicts a phase-sensitive two-dimensional ROESY spectrum where only negative levels are shown. It was recorded for a pure sample of standard material ginsenoside Re This figure was drawn from reference [30] and the readers are strongly encouraged to review the discussion relating to the interpretation of that spectrum as 2-D spectra are, at best, difficult to interpret despite their "nice pictures" appearance.

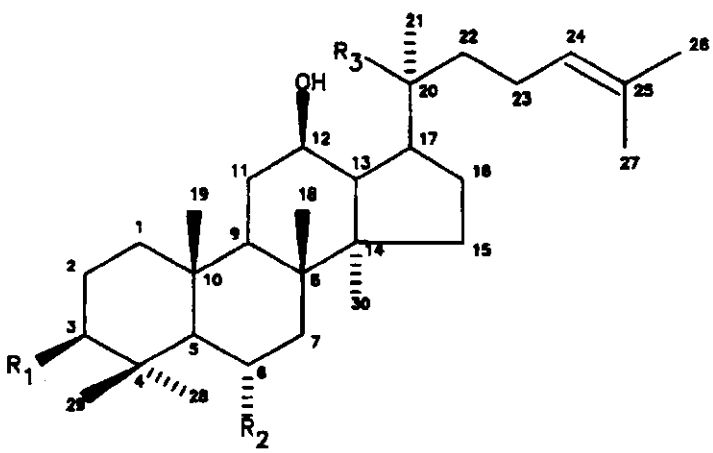

Compound	R1	R2	R3
20S-protopanaxdiol	OH	H	OH
20S-protopanaxtriol	OH	OH	OH
Ginsenoside Rb_1	O-Glcp^{2}-^{1}Glcp	H	O-Glcp^{6}-^{1}Glcp
Ginsenoside Rb_2	O-Glcp^{2}-^{1}Glcp	H	O-Glcp^{6}-^{1}Arap
Ginsenoside Rc	O-Glcp^{2}-^{1}Glcp	H	O-Glcp^{6}-^{1}Araf
Ginsenoside Rd	O-Glcp^{2}-^{1}Glcp	H	O-Glcp
Ginsenoside Re	OH	O-Glcp^{2}-^{1}Rhap	O-Glcp
Ginsenoside Rg_1	OH	O-Glcp	O-Glcp

Figure 26. General structures of the ginsenosides. Glcp = β-D-glucopyranose, Rhap = α-L-rhanmopyranose; Arap = α-L-arabinopyranose; Araf = α-L-arabinofuranose.

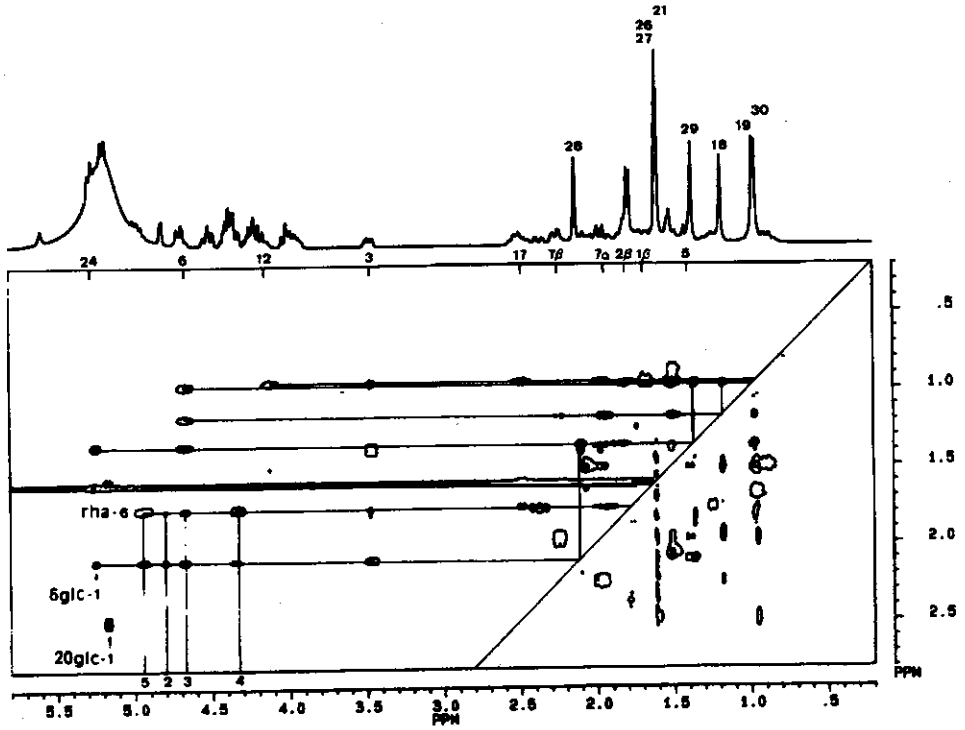

Figure 27. Typical phase-sensitive two-diemnsional ROESY spectrum of ginsenoside Re. Only negative levels are show. Reprinted from reference [30], with permission.

6.9.2 "SNIF-NMR"

Over the years, Site-Specific Natural Isotope Fractionation (SNIF) NMR has been used extensively in food analysis. Deuterium (^2H) is widely dispersed in the whole solar system and so it is as well on earth. Actually, the deuterium isotope ratio ($^2H/^1H$) in water, usually expressed in parts per million (ppm - just to confuse the matter a little more for NMR spectroscopists) ranges between 90 and 160 ppm according to the latitude where the measurement is made (the value increasing from the south pole to the equator). Water being the only source of hydrogen atoms involved in photosynthetic pathways, it follows that "fingerprint" deuterium contents are associated with such various pathways and with their origin. The latter being influenced by the climatic and geographical conditions prevailing at the time where the photosynthesis takes place.

A group or researcher at the Université de Nantes, led by G. J. Martin authored a technical brochure on behalf of Bruker, a NMR instrument manufacturer, that provides good background material on SNIF-NMR [44]. Although the brochure focuses on the "automation of wine NMR" (the term used by the

Table 2
NMR in the analysis of food sample*

Summary of work	NMR techniques reported	Ref.
^{13}C-NMR used to study composition & structure of plant material, including onions and tomatoes.	Pulse excitation; cross-polarisation excitation &magic angle spinning	[62]
Studies on the distribution of short-chain acyl groups between primary & secondary positions of triglycerides in fats, using high-resolution GLC and ^{1}H-NMR.	500-MHz ^{1}H NMR	[63]
The use of NMR to study the moisture content of various food products, including casein [64] butter bean,	^{17}O NMR transverse relaxation rates.	[64]
rigatoni pasta and snack food [65].	Non-invasive NMR imaging (MRI).	[65]
Development of a computerized method to visualize bruises in apples.	Magnetic Resonance Images	[66]
Detection of adulteration in fruit juices.	SNIF/NMR (deuterium) and SIRA/MS (stable isotope ratio analysis/mass spectrometry).	[67]
A validated and collaborative study for the detection of beet sugar in fruit juices.	SNIF-NMRREGISTERED Measurement of deuterium and carbon-13 levels.	[68]
Screening tool for determining the authenticity of orange juice.	^{1}H-NMR	[69]
Determination of oil in oilseeds [70].	Free induction decay (FID), echo signals in a spin-echo pulse sequence.	[70]
Determination of oil and water in oilseeds [71].	Pulsed NMR.	[71]
Studies on production, storage and quality control measures of dairy products including Cheddar, Brie, Danish Blue and Danish Harvarti cheeses, fromage frais and milk [72]	3 NMR imaging methods, *i. e.,*: 2-dimentional spin warp; 3-dimentional missing pulse steady-state free precession; and Dixon chemical shift resolved imaging sequences.	[72]
Monitoring of P-containing ingredients in cheese.	Cross-polarization magnetic angle spinning.	[73]

*A recent book on NMR in food science is also included in our reference list [74].

author to depict the automated analysis of wines (for enrichment or dilution) by NMR), several examples are used to demonstrate the power of NMR in identifying the origin of certain components in foodstuffs (here, for example, ethanol from various sources). A good number of basic references are provided dealing with the methodology used [45], the mechanisms involved [46-51], and applications to wines [52, 53], spirits [54, 55], beer [56], sugars [51, 57], and aromas and essential oils [58-61].

In summary, these applications allow for the positive identification of the origin of material, *e.g.*, wines, with respect to its geographical origin as well as the nature of the ingredients used to make it. This has significant impact on the marketing activities of these products, especially in the high-value added range or for the "appellation d'origine contrôllée". Obviously, the same techniques can be applied for quality control activities at the production site. Hence, it is safe to say that SNIF-NMR is a powerful technique with special value to the food scientists.

6.9.3 Survey of other applications

As per most chapters in this book, we include a short list (Table 2) of selected applications of NMR to food analysis. It will be obvious to those involved in daily use of NMR that these applications are by no means representative of the range of applicability of NMR to food science, rather they were selected for their practicality and their state of readiness of being implemented into daily food analysis activities.

6.10 REFERENCES

1. F. Bloch, W. W. Hansen and M. E. Packard, *Phys. Rev.* **69**, 127 (1946).

2. E. M. Purcell, H. C. Torrey and R. V. Pound, *Phys. Rev.* **69**, 37 (1946).

3. J. A. Pople, W. G. Schneider, and H. J. Bernstein, "High-Resolution Nuclear Magnetic Resonance", McGraw-Hill, New York, (1959).

4. R. R. Ernst, G. Bodenhausen and A. Wokaun, "Principles of Nuclear Magnetic Resonance in One and Two Dimensions", Clarendon Press, Oxford (1990).

5. C. P. Slichter, "Principles of Magnetic Resonance" (3rd edn), Springer-Verlag, Berlin (1990).

6. R. K. Harris, "Nuclear Magnetic Resonance Spectroscopy. A Physicochemical View", Longman, London (1986).

7. M. Goldman, "Quantum Description of High-Resolution NMR in Liquids", Clarendon Press, Oxford (1991).

8. A. Abragam, "The Principles of Nuclear Magnetism", Clarendon Press, Oxford (1986).

9. H. Günther, "NMR Spectroscopy", Wiley, Chichester (1980).

10. H. Friebolin, "Basic One- and Two-Dimensional NMR Spectroscopy", (2nd edn), VCH, Weinheim (1993).

11. J. K. M. Sanders and B. K. Hunter, "Modern NMR Spectroscopy. A Guide for Chemists." (2nd edn), Oxford University Press (1993).

12. R. J. Abraham, J. Fisher and P. Loftus, "Introduction to NMR Spectroscopy", John Wiley & Sons, Chichester (1988).

13. A. E. Derome, "Modern NMR Techniques for Chemistry Research", Pergamon Press, Oxford (1995).

14. P. S. Belton, I. Delgadillo, A. M. Gil and G. A. Webb (Eds.), "Magnetic Resonance in Food Science", Thomas Graham House, Royal Society of Chemistry, Cambridge (1995).

15. M. Karplus, *J. Chem. Phys.* **30**, 11 (1959).

16. L. M. Jackman and F. A. Cotton (Eds.), "Dynamic Nuclear Magnetic Resonance Spectroscopy", Academic Press, New York (1975).

17. J. Sandström, "Dynamic NMR Spectroscopy", Academic Press, New York (1982).

18. M. Oki (Ed.), "Applications of Dynamic NMR Spectroscopy to Organic Chemistry", VCH Publishers, Deerfield Beach (1985).

19. D. Neuhaus and M Williamson, "The Nuclear Overhauser Effect in Structural and Conformational Analysis", VCH Publishers, New York (1989).

20. E. Breitmaier and W. Voelter, "Carbon-13 NMR Spectroscopy. High-Resolution Methods and Applications in Organic Chemistry and Biochemistry", (3rd edn.), VCH, Weinheim (1990).

21. C. Chachaty, Z. Wolkowski, F. Piriou and G. Lukacs, *J. Chem. Soc. Chem. Commun.* 951 (1973).

22. D. Doddrell and A. Allerhand, *J. Amer. Chem. Soc.* **93**, 1558 (1971).

23. C. A. Fyfe, "Solid State NMR for Chemists", CFC Press, Guelph (1983).

24. M. Mehring, "High Resolution NMR in Solids", (2nd edn.), Springer Verlag, New York (1983).

25. B. C. Gerstein and C. R. Dybrowski, "Transient Techniques in NMR of Solids", Academic Press, Orlando (1985).

26. K. Nakanishi (Ed.), "One-dimensional and Two-dimensional NMR Spectra by Modern Pulse Techniques", Kodansha, Tokyo (1990).

27. J. N. S. Evans, "Biomolecular NMR Spectroscopy", Oxford University Press, Oxford (1995).

28. J.-H. Kwon, J. M. R. Bélanger, and J. R. J. Paré, *Radiat. Phys. Chem.* **34**, 953 (1989).

29. J.-H. Kwon, J. M. R. Bélanger, M. Sigouin, J. Lanthier, C. Willemot, and J. R. J. Paré, *J. Agric. Food Chem.* **38**, 830 (1990).

30. M.-R. Van Calsteren, J.-H. Kwon, J. M. R. Bélanger, and J. R. J. Paré, *Spectros. Int. J.* **11**, 117 (1993).

31. D. M. Doddrell, D. T. Pegg, and M. R. Bendall, *J. Magn. Reson.* **48**, 323 (1982).

32. A. Bax and R. Freeman, *J. Magn. Reson.* **44** 542 (1981).

33. U. Piantini, O. W. Sørensen, and R. R. Ernst, *J. Am. Chem. Soc.* **104**, 6800 (1982).

34. A. J. Shaka and R. Freeman, *J. Magn. Reson.* **51**, 169 (1983).

35. D. Marion and K. Wüthrich, *Biochem. Biophys. Res. Commun.* **113**, 967 (1983).

36. M. Rance, O. W. Sørensen, G. Bodenhausen, G. Wagner, R.R. Ernst, and K. Wüthrich, *Biochem. Biophys. Res. Commun.* **117**, 458 (1983).

37. G. Wagner, *J. Magn. Reson.* **55**, 151 (1983).

38. A. Bax and G. Drobny, *J. Magn. Reson.* **61**, 306 (1985).

39. T. H. Mareci and R. Freeman, *J. Magn. Reson.* **51**, 531 (1983).

40. A. A. Bothner-By, R. L. Stephens, J. Lee, D. C. Warren, and R. W. Jeanloz, *J. Am. Chem. Soc.* **106**, 811 (1984).

41. A. Bax and D. G. Davis, *J. Magn. Reson.* **63**, 207 (1985).

42. A. Bax and G. Morris, *J. Magn. Reson.* **42**, 501 (1981).

43. G. A. Pearson, *J. Magn. Reson.* **64**, 487 (1985).

44. G. J. Martin, Deuterium-NMR in the Investigation of Site-Specific Natural Isotope Fractionation (SNIF-NMR), Technical brochure by Bruker Analytische Messtechnik GMBH, No. NMR/A314/188 (1988).

45. G. J. Martin, X. Y. Sun, C. Guillou, and M. L. Martin, *Tetrahedron* 3285 (1985).

46. G. J. Martin, *Terahedron Lett.* **22**, 3525 (1981).

47. G. J. Martin and M. L. Martin, *C. R. Acad. Sci. Paris* **293**, 35 (1981).

48. G. J. Martin, M. L. Martin, F. Mabon, and M. J. Michon, *J. C. S. Chem. Comm.* 616 (1982).

49. G. J. Martin, B. L. Zhang, M. L. Martin, and P. Dupuy, *Biochem. Biphys. Res. Comm.* **111**, 890 (1983).

50. M. L. Martin, B. L. Zhang, and G. J. Martin. *FEBS Lett.* **158**, 131 (1983).

51. G. J. Martin, B. L. Zhang, N. Naulet, and M. L. Martin, *J. Amer. Chem. Soc.* **108**, 5116 (1986).

52. G. J. Martin and M. L. Martin, *J. Chim. Phys.* **80**, 293 (1983).

53. G. J. Martin, C. Guillou, N. Naulet, S. Brun, Y. Tep, J. C. Cabanis, M. T. Cabanis, and P. Sudraud, *Science des Aliments* **6**, 385 (1986).

54. G. J. Martin, M. L. Martin, F, Mabon, and M. J. Michon, *Anal. Chem.* **54**, 2380 (1982).

55. G. J. Martin, M. L. Martin, F, Mabon, and M. J. Michon, *J. Agric. Food Chem.* **31**, 311 (1983).

56. G. J. Martin, M. Benbernou, and F. Lantier, *J. Inst. Brew.* **91**, 242 (1985).

57. G. J. Martin, B. L. Zhang, L. Saulnier, and P. Colonna, *Carboh. Res.* **148**, 132 (1985).

58. G. J. Martin, M. L. Martin, F. Mabon, and J. Bricout, *J. Amer. Chem. Soc.* **104**, 2658 (1982).

59. G. J. Martin, M. L. Martin, F. Mabon, and J. Bricout, *Sci. Technol. Aliments* **3**, 147 (1983).

60. G. J. Martin, P. Janvier, and F. Mabon, *Analysis* **13**, 267 (1985).

61. G. J. Martin, P. Janvier, S. Akoka, F. Mabon, and J. Jurczak, *Tetrahedron Lett.* **27**, 2855 (1986).

62. T. J. Foster, S. Ablett, M. C. McCann, and M. J. Gidley, *Biopolymers* **39**, 51 (1996).

63. P. Kalo, A. Kemppinen, and I. Kilpelainen, *Lipids* **31**, 331 (1996).

64. A. Mora-Gutierrez, H. M. Farrell Jr., and T. F. Kumosinski, *J. Agric. Food Chem.* **44**, 796 (1996).

65. S. L. Duce and L. D. Hall, *J. Food Eng.* **26**, 251 (1995).

66. B. Zion, P. Chen, and M. J. McCarthy, *Comp. Electro. Agric.* **13**, 289 (1996).

67. G. G. Martin, V. Hanote, M. Lees, and Y. L. Martin, *J. AOAC Int.*, **79**, 62 (1996).

68. G. Martin, *Fruit Processing* **5**, 246 (1995).

69. J. T. W. E. Vogels, L. Terwel, A. C. Tas, F. van den Berg, F. Dukel, and J. van der Greef, *J. Agric. Food Chem.* **44**, 175 (1996).

70. P. N. Tiwari and P. N. Gambhir, *J. Amer. Oil Chem. Soc.* **72**, 1017 (1995).

71. G. Rubel, *J. Amer. Oil Chem. Soc.* **71**, 1057 (1994).

72. S. L. Duce, M. H. G. Amin, M. A. Horsfield, M. Tyszka, and L. D. Hall, *Int. Dairy J.* **5**, 311 (1995).

73. L. T. Kakalis, T. F. Kumosinski, and H. M. Farrell Jr., *J. Dairy Sci.* **77**, 667 (1994).

74. P. S. Belton, I. Delgadillo, A. M. Gill, and G. A. Webb (eds), *Magnetic Resonance in Food Science*, Thomas Graham House, Cambridge, UK, 294 pp. (1995).